Studies on the Tumor-Suppressing Activity of Bevacizumab, a Monoclonal Antibody against Human Vascular Endothelial Growth Factor

January 2011

Mieko YANAGISAWA

Studies on the Tumor-Suppressing Activity of Bevacizumab, a Monoclonal Antibody against Human Vascular Endothelial Growth Factor

A Dissertation Submitted to
the Graduate School of Life and Environmental Sciences,
the University of Tsukuba
in Partial Fulfillment of the Requirements
for the Degree of Doctor of Philosophy in Science
(Doctoral Program in Functional Biosciences)

Mieko YANAGISAWA

Contents

Abstract

For tumor cells to proliferate, blood vessels are necessary to supply sufficient nutrition and oxygen. Folkman has suggested that tumor growth is angiogenesis-dependent (Folkman 1990). Vascular endothelial growth factor (VEGF) is an important factor in tumor angiogenesis and growth. VEGF is overexpressed in tumor cells compared to other normal organs. Hypoxia in tumor triggers tumor cells to secrete VEGF which induces angiogenesis by signaling to the VEGF receptor (VEGFR) in normal blood vessels surrounding the tumor. Chemotherapeutic agents have been used for a long time for cancer therapy. However, they have caused severe side-effects because the activity of the chemotherapeutic agents was not specific to tumors. Recently many molecular targeted agents, which are specific to molecular targets genetically amplified or overexpressed in tumor cells, were discovered to reduce side-effects and to improve the efficacy of cancer therapy. These molecular targeted agents were now used with conventional therapies to improve the response. Bevacizumab (BV) is the first molecular targeted agent for VEGF. In this study I investigated the role of VEGF-VEGFR signaling in tumor growth suppression and angiogenesis using BV in human cancer xenograft models.

BV is used worldwide in combination with standard chemotherapies for patients with colorectal cancer, lung cancer and breast cancer. It has been reported that BV in combination with paclitaxel (PTX) significantly prolonged progression-free survival compared with PTX alone in initial treatment for metastatic breast cancer. However, it is not clear why BV enhances the efficacy of the chemotherapeutic agents. To understand the mechanisms of the effects of combination treatments, I tried to establish animal model showing antitumor activity of BV alone and in combination with chemotherapeutic agents such as capecitabine (Cape) or capecitabine plus oxaliplatin (Cape-Oxali). Tumor-inoculated nude mice were treated with BV, Cape, and oxaliplatin alone or in combination, after tumor growth was confirmed. Tumor volume and microvessel density (MVD) in tumor were evaluated. I measured thymidine phosphorylase (TP) and VEGF levels, which were determinants for efficacy of Cape and BV, respectively. BV alone showed significant antitumor activity as in three xenograft models (COL-16-JCK, COLO 205, and CXF280). The MVD in tumors treated with BV was lower than that of the control. Antitumor activity of BV in combination with Cape was significantly higher than that of each agent alone (COL-16-JCK, COLO 205). Furthermore, the antitumor activity of BV in combination with Cape-Oxali was significantly superior to that of Cape-Oxali (COL-16-JCK). TP and VEGF levels were not increased by BV alone and Cape alone, respectively, suggesting there were other potentially efficacious mechanisms involved.

There was a hypothesis that the reduction in vascular permeability in the tumors, which was increased by overexpressed VEGF, induced decrease of interstitial fluid pressure and, consequently,

chemotherapeutic agents were transferred abundantly to tumor cells in combination therapy of BV with chemotherapeutic agents (Jain, 2001; Gerber and Ferrara, 2005). However, there have been no reports that verify the entire processes actually occur. Therefore, I attempted to investigate that point using my animal models. In an MX-1 human breast cancer xenograft model which shows synergistic antitumor activity, the antitumor activity of BV at 5 mg/kg in combination with PTX at 30 mg/kg was significantly higher than that of either agent alone. I measured the PTX concentration in tumors to see whether BV enhances the activity by increasing the tumor concentration of PTX. When given in combination with BV, the level of PTX in tumor increased. PTX at 30 mg/kg with BV showed a similar tumor concentration to PTX alone at either 60 or 100 mg/kg, with a similar degree of tumor growth inhibition. In addition, terminal half-life ($T_{1/2}$) of PTX in the paclitaxel plus bevacizumab (PTX-BV) group was prolonged compared to that in the PTX alone group. No remarkable differences in PTX concentration in plasma or liver were observed between the PTX alone group and the PTX-BV group. In the same MX-1 breast cancer model, vascular permeability in tumor was significantly decreased by treatment with BV. There was no difference in MVD between the BV alone group and the combination group. These results suggest that the synergistic antitumor activity of PTX and BV can be attributed to the increase in PTX concentration in tumors caused by the decrease of vascular permeability and possibly by the $T_{1/2}$ prolongation of PTX. There are two possible explanations as to why the $T_{1/2}$ of PTX is prolonged. One is the decrease of MVD caused by BV, which in turn lessens the PTX return to the vessels and therefore increases the concentration of PTX in tumor cells. The second is the decrease of lymphatic vessel. Although it has long been considered that stimulation of VEGFR-3 induces the formation of the lymphatic vessel system, a recent report has suggested that VEGF-A, VEGFR-2 and neuropilin also function in lymphatic vessel formation (Cueni and Detmar, 2006). Because BV binds to and inactivate VEGF-A, lymphatic vessel formation in tumor should be decreased in the presence of BV and less PTX returns to the vessels. Further experiments are necessary to investigate these possibilities.

Abbreviations

BC	breast cancer
BV	bevacizumab
Cape	capecitabine
Cape-BV	capecitabine plus bevacizumab
Cape-Oxali	capecitabine plus oxaliplatin
C_{max}	maximum drug concentration
CRC	colorectal cancer
EGFR	epidermal growth factor receptor
FGF	fibroblast growth factor
FITC	fluorescein isothiocyanate
FOLFOX4	5-fluorouracil, leucovorin plus oxaliplatin
5-FU	5-fluorouracil
HPLC	high-performance liquid chromatography
HuIgG	human immunoglobulin G
IFP	interstitial fluid pressure
i.p.	intraperitoneally
i.v.	intravenously
MTD	maximum tolerant dose
MVD	microvessel density
NSCLC	non-small cell lung cancer
Oxali	oxaliplatin
p.o.	per os
PTX	paclitaxel
PTX-BV	paclitaxel plus bevacizumab
$T_{1/2}$	terminal half-life time
TGI%	percentage of tumor growth inhibition
T_{max}	maximum drug concentration time
TP	thymidine phosphorylase
VEGF	vascular endothelial growth factor
VEGFR	vascular endothelial growth factor receptor
VPF	vascular permeability factor

General Introduction

The number of cancer patients is increasing every year. Although the total number of patients was ranked 4th out of all diseases in Japan, cancer deaths ranked first and reached approximately 340,000 in 2008 according to the Health, Labour and Welfare Ministry report (http://www.mhlw.go.jp/toukei/saikin/hw/jinkou/kakutei08/). How to treat cancer is one of the major issues still to be resolved in modern medicine. Generally, patients with cancer undergo excision of the tumor in the first treatment and they are given radiation therapy, chemotherapy and hormone treatment in the metastasis phase. Conventional cancer treatments such as cytotoxic chemotherapy and radiation therapy have been developed based upon the observation that malignant cells divide at a more rapid rate than normal cells. For example, radiation induces DNA damage that, upon multiple cell divisions, may lead to errors in transcription and translation resulting in cell death (Rydberg, 2001). The use of chemotherapeutic agents against malignant tumors is successful in many patients but suffers from major drawbacks such as the lack of selectivity to tumor, which sometimes leads to severe side-effects and may limit efficacy.

To reduce the side-effects and to improve the efficacy of cancer therapy, a lot of target based medicines have been developed. Several classes of proteins genetically amplified or overexpressed on the surface of tumor cells, such as epidermal growth factor receptor (EGFR; ErbB-1), ErbB-2, ErbB-3, vascular endothelial growth factor (VEGF) and so on, can be selectively targeted (Pérez-Soler, 2004; Normanno *et al.*, 2003). EGFR are among the most often targeted proteins and their implication in the pathogenesis and evolution of cancer has been clearly established (Mass, 2004; Ronellenfitsch *et al.*, 2010). Antibodies and small molecule inhibitors are selectively targeted to block the action of growth factors. To date, a lot of agents specific to molecular targets have been generated (Fig. 1), including bevacizumab (BV, Avastin®) whose tumor-suppressing activity was investigated in this study. BV is a humanized antibody against VEGF and prevents its binding to the receptor (VEGFR), thereby neutralizing the VEGF activity.

Since the early 1900's, observation that tumor growth can be accompanied by increased vascularity has been reported. In 1928, the introduction by Sandison of a transparent chamber that could be inserted into rabbit ear to allow microscopic observation of living tissue underneath a glass coverslip, provided a tool for experimental and conceptual advances in the field (Sandison, 1928). In 1939, Ide *et al.* used the transparent chamber and investigated the correlation between growth of transplanted rabbit carcinoma and vascular supply. They observed that tumor growth was accompanied by the rapid and extensive formation of new vessels to deliver nutrients to the growing tumor. They also pointed out that if blood-vessel growth did not occur, the transplanted tumor failed to grow (Ide *et al.*, 1939). In 1968, it was reported that transplantation of melanoma or

choriocarcinoma cells prompted blood-vessel proliferation even when a filter was interposed between the tumor and the host (Greenblatt and Shubick, 1968; Ehrmann and Knoth, 1968), indicating that tumor angiogenesis was mediated by diffusible factors produced by tumor cells. Folkman has suggested that tumor growth is angiogenesis-dependent and proposed that anti-angiogenesis might be an effective therapeutic strategy to treat cancer (Folkman 1971). Then, isolation of tumor angiogenesis factor from human and animal tumors (Folkman *et al*., 1971) and from cultured cells (Klagsbrun *et al.*, 1976) was reported. Several angiogenic factors, such as fibroblast growth factor (FGF), angiogenin, transforming growth factor, were also discovered (Folkman and Klagsbrun, 1987). In 1983, Sengar reported the partial purification of vascular permeability factor (VPF), a protein that induced vascular leakage in the skin, from the conditioned medium of a guinea-pig tumor cell line. In 1989, Ferrara and Henzel (1989) reported the isolation of VEGF, an endothelial-cell-specific mitogen, from the culture medium conditioned by bovine pituitary follicular cells. The amino-terminal amino-acid sequence of VEGF did not match any known protein in available databases. After that, Connolly *et al*. (1989) reported the isolation and sequence of human VPF. Isolation of cDNA clones for VEGF (Ferrara and Henzel, 1989), and for VPF (Connolly *et al*., 1989) revealed that VEGF and VPF were the same molecule.

VEGF is an important factor in tumor angiogenesis and growth (Ferrara *et al.*, 1992; Ferrara and Davis-Smith, 1997; Ferrara, 2004; Hoeben *et al*., 2004). VEGF is a heparin binding growth factor with a molecular weight of 45,000, and is as dimeric protein composed of two identical subunits (Ferrara and Henzel, 1989). Six subtypes of VEGF, VEGF-A, -B (Olofsson *et al.*, 1996), -C (Joukov *et al*., 1996), -D (Achen *et al.*, 1998), -E (Ogawa *et al.*, 1998), and -F (Suto *et al*., 2005) and three receptors, VEGFR-1, -2 and -3 (Dai and Rabie, 2007; Otrock *et al*., 2007), are known. The human VEGF-A gene is organized in eight exons (Houk *et al*., 1991; Tischer *et al*., 1991). Alternative exon splicing results in the generation of four main VEGF isoforms, having , respectively 121, 165, 189 and 206 amino acids following signal sequence cleavage ($VEGF_{121}$, $VEGF_{165}$, $VEGF_{189}$, and $VEGF_{206}$) (Leung *et al*., 1989). Hypoxia in tumor triggers tumor cells to secrete VEGF which induces angiogenesis by signaling through VEGFR in a normal blood vessel surrounding the tumor. VEGF mRNA expression is increased by hypoxia inducible factor 1, which is induced by exposure to low pO_2 in a variety of pathophysiological circumstances (Semenza 2003; Ke and Costa, 2006). The VEGF-VEGFR interactions and their consequences are schematically shown in Fig. 2. Each VEGF subtype binds to multiple VEGFR. Activation of VEGFR-1 results in angiogenesis and migration of hematopoietic cells, of VEGFR-2, angiogenesis and permeability increase (Shibuya *et al*., 2006), and of VEGFR-3, lymphatic formation (Karkkainen *et al*., 2002).

It has been reported that VEGF is overexpressed in most human tumors (Ferrara and Davis-Smyth, 1997; Hanrahan *et al*., 2003) to result in tumor microvasculature, disorganization and

lack of the conventional hierarchy of blood vessels by which arterioles, capillaries, and venules become unidentifiable (Hashizume *et al.*, 2000; Carmeliet, 2003; Jain, 2003; McDonald and Choyke, 2003). In the tumor vessels, permeability is increased by VEGF and the plasma constituent leaks easily out of the blood vessel (Ferrara *et al.*, 1992; Ferrara and Davis-Smyth, 1997; Ferrara, 2004).

BV is a genetically-engineered humanized monoclonal antibody derived from murine anti-human VEGF monoclonal antibody A4.6.1. The parental antibody A4.6.1 belongs to IgG1 isotype and its dissociation constant to $VEGF_{165}$ is $8x10^{-10}$ M. A4.6.1 specifically recognized VEGF but not to platelet-derived growth factor, which has a 15-18% sequence homology to VEGF (Leung *et al.*, 1989), and other growth factors such as epidermal growth factor, acidic FGF, nerve growth factor and hepatocyte growth factor (Kim *et al.*, 1992). BV is 93% human and 7% murine protein sequence, producing an agent with the same biochemical and pharmacologic properties as the parental antibody (Kim *et al.*, 1992; Presta *et al.*, 1997). In common with A4.6.1, BV binds to and neutralizes all human VEGF-A isoforms and their bioactive proteolytic fragments. The binding epitope of BV has been defined by crystal structure analysis of a Fab-ligand complex (Müller *et al.*, 1998). This analysis predicts that Gly88 in human VEGF is essential for binding BV and this residue also underlines the species specificity of BV binding, since serine residue is found in mouse and rat VEGF at the corresponding position (Ferrara *et al.*, 2004). BV specifically binds to human VEGF-A, thereby blocking the binding of VEGF-A to VEGF receptors expressed on vascular endothelial cells. By blocking the biological activity of VEGF (Wang *et al.*, 2004), BV, or its murine equivalent A4.6.1, inhibits neovascularization in tumors and thus suppresses tumor growth in xenograft models (Kim *et al.*, 1993; Presta *et al.*, 1997; Gerber and Ferrara, 2005; Warren *et al.*, 1995).

BV was first approved for colorectal cancer in the US in 2004. Since then, it has been used worldwide in combination with standard chemotherapies for patients with colorectal cancer (CRC), non-small cell lung cancer (NSCLC) and breast cancer (BC). In Japan, BV was approved for therapy of CRC and NSCLC in 2007 and 2009, respectively. In the evaluation of cancer treatment, ‘progression-free survival’ and ‘response rate’ are used as markers how well a new treatment works. ‘progression-free survival’ is the term during and after treatment in which a patient is living with a disease that does not get worse. ‘Response rate’ is the percentage of patients whose cancer shrinks or disappears after treatment. BV in combination with chemotherapeutic agents significantly prolonged progression-free survival and increased the response rate compared with chemotherapy alone in patients with CRC, NSCLC and BC (Hurwitz *et al.*, 2004; Kabbinavar *et al.*, 2003; Sandler *et al.*, 2006; Miller *et al.*, 2007).

In Chapter I of this study, I evaluated the antitumor activity of BV in human colorectal cancer xenograft models, both as a monotherapy and in combination with capecitabine (Cape) alone and with capecitabine plus oxaliplatin (Cape-Oxali) which were chemotherapeutic agents used as

first-line therapy for colorectal cancer patients. To understand the mechanisms of the effects of the combination of capecitabine plus bevacizumab (Cape-BV), I measured the levels of thymidine phosphorylase (TP) and VEGF, which are determinants for efficacy of Cape and BV, respectively.

The synergistic effects of BV with chemotherapy have been attributed to a reduction in vascular permeability with normalization of the vasculature by obstructing the VEGF-VEGFR signaling. Vascular permeability reduction causes decrease of interstitial fluid pressure (IFP), and consequently, chemotherapeutic agents are transferred abundantly to tumor cells in combination therapy of BV with chemotherapeutic agents (Jain, 2001; Gerber and Ferrara, 2005). However, there is no report that verifies all of these processes. A demonstration of all the processes is required to clarify why BV with chemotherapeutic agents shows synergistic effects. In Chapter II of this study, I examined the synergistic antitumor activity of combination therapy of paclitaxel (PTX) and BV in a human breast cancer xenograft model, and also investigated the effect of BV on PTX concentration and the blood vessel permeability in the model.

Chapter I

Tumor-suppressing activity of bevacizumab in combination with capecitabine and oxaliplatin in human colorectal cancer xenograft models

Introduction

BV (Avastin®) is a genetically engineered humanized monoclonal antibody derived from murine anti-human VEGF monoclonal antibody A4.6.1 (Presta *et al*., 1997; Kim *et al*., 1992). It binds specifically to human VEGF, thereby blocking the binding of VEGF to VEGF receptors expressed on vascular endothelial cells. By blocking the biological activity of VEGF (Wang *et al*., 2004), BV or its murine equivalent A4.6.1 inhibits neovascularization in tumors and thus suppresses tumor growth (Presta *et al*., 1997; Kim *et al*., 1993; Gerber and Ferrara, 2005). Clinically, it has been reported that BV significantly improved the survival benefit among patients with metastatic colorectal cancers in combination with irinotecan hydrochloride, 5-fluorouracil (5-FU), and leucovorin and with 5-FU and leucovorin (Hurwitz *et al*., 2004; Kabbinavar *et al*., 2003).

Cape (N^4-pentyloxycarbonyl-5'-deoxy-5-fluorocytidine, Xeloda®) is an oral fluoropyrimidine drug widely used. It is converted first to 5'-deoxy-5-fluorocytidine by carboxylesterase located in the liver, then to 5'-deoxy-5-fluouridine by cytidine deaminase expressed in the liver and various solid tumors, and finally to 5-FU by TP highly expressed in many tumors. It has been reported that the antitumor activity of Cape correlates with tumor levels of TP activity in xenograft models (Ishikawa *et al*., 1998). A recent clinical study has reported that the combination therapy of BV with FOLFOX4 (5-fluorouracil, leucovorin plus oxaliplatin) or with Cape-Oxali significantly improves progression free survival compared with FOLFOX4 or Cape-Oxali alone in first-line metastatic colorectal cancer (Saltz *et al*., 2008).

In my present study, I evaluated the microvessel density (MVD) decrease by BV and antitumor activity of BV as a monotherapy and in combination with Cape alone and with Cape-Oxali in human colorectal cancer xenograft models. To understand the mechanisms of the effects of the combination of Cape-BV, I measured the levels of TP and VEGF, which are determinants for efficacy of Cape and BV, respectively.

Materials and Methods

Animals

Five-week-old male BALB-nu/nu (CAnN.Cg-Foxn1<nu>/CrlCrlj nu/nu) mice were obtained from Charles River Laboratories Japan, Inc. (Kanagawa, Japan) and acclimatized for at least 1 week in our animal facility before use. The number of animals per experiment group was four to six, as specified in the figures. All animal experiments were conducted in accordance with the 'Standards for the Care and Management of Experimental Animals' and 'Rules for Animal Care and Management' promulgated in Chugai Pharmaceutical Co., Ltd.

Tumors

Three human colorectal cancer lines were used in this study. COL-16-JCK was provided by the Central Institute for Experimental Animals (Kanagawa, Japan), COLO 205 (ATCC CCL-222) was purchased from American Type Culture Collection (Manassas, VA, USA) and CXF280 was kindly provided by Dr H.H. Fiebig (University of Freiburg, Freiburg, Germany). COL-16-JCK and CXF280 were maintained in BALB-nu/nu mice by subcutaneous inoculation of tumor pieces. COLO 205 was maintained in vitro in culture medium RPMI-1640 containing 2 mM L-glutamine, 10 mM HEPES, 1 mM sodium pyruvate, 4.5 g/l glucose, 1.5 g/l sodium bicarbonate and 10% FBS at 37˚C in an incubator with 5% CO_2.

Human Colorectal Cancer Xenograft Models

Pieces (~2 x 2 mm) of minced tumor of COL-16-JCK and CXF280 were inoculated subcutaneously (s.c.) into the right flank region of male BALB-nu/nu mice. A suspension of COLO 205 cells (5×10^6 or 8.8×10^6 viable cells/mouse) was injected s.c. into a male BALB-nu/nu mouse. Treatments with the antitumor drugs were started after tumors were sufficiently established in the mice. Tumor volume was estimated using the equation $V = ab^2/2$, where a and b are tumor length and width, respectively. The percentage of tumor growth inhibition (TGI%) was calculated as follows: TGI% = [1-(Mean change in tumor volume in each group treated with antitumor drugs/Mean change in tumor volume in the control group)] x 100.

Immunohistochemistry

Tumors were collected after treatment with BV or human immunoglobulin G (HuIgG). Immunohistochemistry was performed using the standard method of avidin-biotin complex peroxidase staining on 4-μm thick sections from paraffin-embedded, formalin-fixed tissue. The CD34 antibody (rat monoclonal antibody, clone MEC14.7; HyCult Biotechnology, Uden, The

Netherlands) (Garlanda *et al*., 1997) was used to identify the microvessels.

MVD

MVD was determined as the ratio of the CD34-positive area to the total observation area. Four to six fields per section (0.4977 mm^2 each) were randomly analyzed, excluding necrotic areas. The CD34-positive areas within the viable regions were measured using imaging analysis software Win ROOF (Mitani Corporation, Fukui, Japan).

TP levels in the tumor

Tumors were homogenized in 10 mM Tris-buffer (pH 7.4) containing 15 mM NaCl, 1.5 mM $MgCl_2$ and 50 μM potassium phosphate buffer using a glass homogenizer. The homogenizer was then centrifuged at 10,000 rpm for 15 min at 4˚C and the supernatants were stored at -80˚C until use. The protein concentration of the supernatants was determined using a DC protein assay kit (Bio-Rad, Hercules, CA, USA). The level of TP was measured by ELISA with monoclonal antibodies specific to human TP, as previously described by Nishida *et al* . (Nishida *et al*., 1996). One unit corresponds to the amount of TP enzyme activity, which phosphorylates 5'-DFUR to 5-FU at rate of 1 μg 5-FU per hour (recombinant human TP).

Levels of VEGF in tumors

Tumors were homogenized in PBS buffer containing 0.05% Tween-20 using a glass homogenizer. The homogenized samples were then centrifuged at 10,000 x g for 20 min at 4˚C and the supernatants were stored at -80˚C until use. The protein concentration of the supernatants was determined using a DC protein assay kit (Bio-Rad). The level of VEGF was measured using a human VEGF ELISA kit (R&D, Minneapolis, MN, USA).

Chemicals

BV (Avastin®) and Cape (Xeloda®) were obtained from F. Hoffman-La Roche Ltd. (Basle, Switzerland). Oxaliplatin (Oxali) was kindly provided by Sanofi-Synthelabo Inc. (presently Sanofi-Aventis). HuIgG was purchased from MP Biomedicals, Inc. (Solon, OH, USA). BV and HuIgG were diluted with saline and administered intraperitoneally (i.p.) twice a week for 3 weeks. Cape was suspended in 40 mM citrate buffer (pH 6.0) containing 5% gum arabic as the vehicle and given orally (per os, p.o.) for 14 days. Oxali was dissolved in 5% glucose solution and given intravenously (i.v.) once only on the day of treatment initiation.

Statistical analysis

Statistical analysis was performed using the Mann-Whitney U test. Differences were considered to be significant for values of $P < 0.05$.

Results

Tumor growth inhibition by BV alone

I examined the antitumor activity of BV alone in three human colorectal cancer xenograft models. A piece of minced COL-16-JCK tumor was inoculated s.c. into the right flank region of BALB-nu/nu mice. Twenty-one days after tumor inoculation, the mice were divided into 4 groups and treatment was initiated (Day 1). BV at doses of 1.2, 2.5 and 4.0 mg/kg and HuIgG at 4.0 mg/kg as the control were administered i.p. twice a week for 3 weeks. Antitumor activity was evaluated on Day 22 (21 days after the treatment was initiated). TGI% was 46, 59 and 55% in the groups treated with BV at 1.2, 2.5 and 4.0 mg/kg, respectively. There were statistically significant differences in tumor volume between the control group and the groups treated with BV at doses of 1.2 mg/kg or above ($P < 0.05$, Fig. 3a).

BALB-nu/nu mice were injected s.c. with 5×10^6 cells of COLO 205 cell line into the right flank region. Nine days after the injection of the tumor cells, treatment was started. TGI% on Day 22 was 33, 41 and 44% in the groups treated with BV at doses of 1.2, 2.5 and 4.0 mg/kg, respectively. There were statistically significant differences in tumor volume between the control group and the groups treated with BV at doses of 1.2 mg/kg and above ($P < 0.05$, Fig. 3b).

For mice inoculated with CXF280, treatment was initiated 18 days after inoculation. TGI% on Day 22 was 22, 40 and 47% in the groups treated with BV at doses of 0.4, 1.2 and 4.0 mg/kg, respectively. There were statistically significant differences in tumor volume between the control group and the groups treated with BV at doses of 1.2 mg/kg and above ($P < 0.05$, Fig. 3c). No significant decrease in body weight was observed in any of the groups of the three xenograft models (Fig. 3a, b and c).

Antitumor activity of BV in combination with Cape

I evaluated the antitumor activity of BV in combination with Cape in two human colorectal cancer xenograft models. Twenty-seven days after inoculation with COL-16-JCK tumors, the mice were divided into 4 groups (6 mice per group) and treatment was initiated (Day 1). BV was administered i.p. at 4 mg/kg twice a week for 3 weeks and Cape was orally administered at 359 mg/kg [2/3 maximum tolerated dose (MTD)] (Ishikawa *et al*., 1998) daily for 14 days. On Day 37, there were statistically significant differences in tumor volume between the control and the groups treated with Cape alone, BV alone and Cape-BV. There were also statistically significant differences in tumor volume between the group treated with Cape-BV and the groups treated with BV alone and Cape alone ($P < 0.05$, Fig. 4). TGI% on Day 37 was 52% in the Cape alone group, 35% in the BV alone group and 80% in the Cape-BV combination group.

COLO 205 colorectal cancer cells (8.8×10^6) were injected s.c. into the right flank region of BALB-nu/nu mice. Seven days after tumor cell injection, the mice were divided into 4 groups (6 mice per group) and treatment was initiated (Day 1). BV was administered i.p. at 4 mg/kg twice a week for 3 weeks. Cape was administered p.o. at 269 mg/kg [1/2 MTD (Ishikawa *et al*., 1998)] daily for 14 days. Tumor volumes on Day 22 were significantly smaller in the Cape-BV group than in groups treated with each agent alone ($P < 0.05$, Fig. 5). TGI% was 55% in the Cape group, 44% in the BV group and 82% in the Cape-BV combination group.

No significant difference in body weight was observed between mice treated with Cape-BV and those treated with each single agent in the COL-16-JCK and COLO 205 models (Figs. 4 and 5).

Antitumor activity of BV in combination with Cape-Oxali

The mice inoculated with COL-16-JCK were divided into 6 groups (6 mice per group); 25 days after tumor inoculation treatments were initiated (Day 1). Cape was administered p.o. at 180 mg/kg (1/3 MTD) (Ishikawa *et al*., 1998) daily for 14 days. Oxali was administered i.v. at 5 mg/kg (1/3 MTD) (Sawada *et al*., 2007) on Day 1 and 4 mg/kg of BV was administered i.p. twice a week for 3 weeks. On Day 36, Cape and Oxali significantly inhibited tumor growth as single agent. TGI% was 38% in the Cape alone group, 23% in the Oxali alone group and 70% in the Cape-Oxali group (Fig. 6). Cape in combination with Oxali showed significantly higher antitumor activity than Cape, although Oxali as a single agent showed no significant antitumor activity. Furthermore, tumor volume of BV in combination with Cape-Oxali group was significantly smaller than that of Cape-Oxali group and BV alone group. TGI% was 86% in the BV in combination with Cape-Oxali group, 70% in the Cape-Oxali group and 44% in the BV alone group. No significant difference in body weight was observed between mice treated with Cape-Oxali alone and those treated with Cape-Oxali plus BV (Fig. 7).

Effect of BV on MVD

I investigated the effect of BV on MVD in tumors of the COL-16-JCK xenograft model by using immunohistochemical staining for CD34. BV at doses of 1.2 and 4.0 mg/kg and HuIgG at 4.0 mg/kg as a control were administered i.p. twice a week for 3 weeks (41 days post-tumor inoculation). Tumors were collected 5 days after the last treatment (Day 23). TGI% was, respectively, 43 and 45% in the groups treated with BV at 1.2 and 4.0 mg/kg on Day 23. Typical immunohistochemical staining images of CD34 are shown in Fig. 8. The MVD was determined as the ratio of the CD34-positive area to the total observation area and were 1.00, 0.70 and 0.51% at the dosages of 0 (control), 1.2, and 4.0 mg/kg of BV, respectively; MVD values were significantly lower for the BV-treated groups than for the control group ($P < 0.05$, Fig. 9).

Levels of TP and VEGF in tumor

I measured the levels of TP and human VEGF in tumors in COL-16-JCK and COLO 205 xenograft models. Levels of tumor TP were not changed after i.p. administration of BV at 4 mg/kg twice a week for 3 weeks in the COL-16-JCK and COLO 205 xenograft models. The level of VEGF in tumor was not increased by Cape treatment (539 mg/kg, daily for 13 days) in the COL-16-JCK model (Table 1).

Discussion

In my present study, I demonstrated the antitumor activity of BV alone, Cape-BV and Cape-Oxali plus BV in human colorectal cancer xenograft models. The antitumor activity of BV in combination with Cape was significantly higher than that of BV alone in 2 xenograft models. In addition, I investigated the mechanisms of the combination effects of BV and Cape in the 2 xenograft models.

Cape is enzymatically metabolized to 5-FU as a result of the highly expressed TP in the tumor. It has been reported that the antitumor activity of Cape correlates with tumor levels of TP activity in xenograft models (Ishikawa *et al*., 1998). Some chemotherapeutic drugs, such as the taxanes, have been reported to increase the levels of TP in tumors in xenograft models and to show significantly more potent antitumor activity in combination with Cape than each agent alone (Sawada *et al*., 1998; Endo *et al*., 1999; Ishitsuka *et al*., 1996). It has been also reported that Oxali treatment increased the level of TP in tumors in xenograft models (Sawada *et al*., 2007). In the present study, I investigated the levels of TP in tumors after treatment with BV to evaluate possible therapeutic effects in combination with Cape and with Cape-Oxali in xenograft models. However, BV induced no significant increase in levels of TP in the 2 xenograft models used, suggesting that the combination effects are a result of mechanisms other than TP up-regulation in tumors treated with BV. A4.6.1 has been reported to increase pO_2 in tumors (Lee *et al*., 2000). On the other hand, hypoxia has been reported to induce TP in tumor cells (Akiyama *et al*., 2004) and might explain the lack of an increase in the levels of TP in the tumor after treatment with BV in the xenograft models tested.

BV binds to human VEGF and inhibits its biological activities. VEGF has been reported to be expressed in tumors and to play a major role in tumor angiogenesis (Ferrara and Henzel, 1989; Leung *et al*., 1989; Ferrara, 2004). As in many studies, the present study also demonstrated that BV decreased MVD in the tumors of the xenograft models. In tumors expressing VEGF, tumor growth would be more dependent on angiogenesis regulated by VEGF. Therefore, I investigated the level of VEGF after treatment with Cape to possibly explain the mechanisms of the effects of Cape-BV combination. However, no significant increase in tumor VEGF was demonstrated after treatment with Cape, suggesting that the combination effects are a result of mechanisms other than change in the level of VEGF in tumors treated with Cape.

In the present study using human colorectal cancer xenograft models, I investigated the possible mechanisms explaining the clinical benefits demonstrated in a clinical study of combination therapy of BV with Cape-Oxali in colorectal cancer patients. The levels of TP and VEGF measured in tumor, however, did not explain the mechanism of the effects of the combination demonstrated in xenograft

models. Previously, A4.6.1 has been shown to increase the concentration of anticancer agents in the tumors as compared with anticancer agents alone (Wildiers *et al*., 2003). I will further investigate the mechanisms of combination therapies plus BV in xenograft models that show effects of antitumor activity.

Chapter II

Tumor-suppressing activity of bevacizumab and its effect on drug delivery

Introduction

BV in combination with PTX is approved as first-line therapy in patients with metastatic breast cancer in EU in 2007 and in the US in 2008. In Japan, BV treatment for BC was applied for Health, Labour and Welfare Ministry approval and now it is under the evaluation. PTX binds to ß-tubulin and stabilizes microtubules, repressing the dynamic instability of spindle microtubules, and thus results in blocking the cell cycle at the metaphase-to-anaphase transition (Horwitz, 1992). It is used for breast cancer treatment as a chemotherapeutic agent in combination with other chemotherapeutic agents or molecular targeted agents. Paclitaxel plus bevacizumab (PTX-BV) significantly prolonged progression-free survival as compared with PTX alone and increased the response rate (Miller *et al.*, 2007), although the mechanisms of the combination therapy are still elusive.

In my present study, I attempted to demonstrate the synergistic antitumor activity of combination therapy with PTX-BV and to investigate the mechanism of the combination therapy in an MX-1 human breast cancer xenograft model. As it has been hypothesized that BV may enhance the delivery of chemotherapeutic agents to tumors as a result of the normalization of tumor vessels resulting from the decrease of vascular permeability (Jain, 2001; Gerber and Ferrara, 2005), I compared the concentrations of PTX in tumors treated with PTX in combination with BV and in those treated with PTX alone. I also examined vascular permeability in tumors.

Materials and Methods

Animals

Five-week-old female BALB-nu/nu (CAnN.Cg-Foxn1<nu>/CrlCrlj nu/nu) mice for the MX-1 xenograft model and male BALB-nu/nu mice for the A549 xenograft model were obtained from the Charles River Laboratories, Inc. (Kanagawa, Japan). The mice were acclimatized for at least 1 week in our animal facility before use. All the animal experiments were conducted in accordance with the Institutional Animal Care and Use Committee in Chugai Pharmaceutical Co., Ltd.

Human cancer xenograft model

The MX-1 human breast cancer cell line was provided by Dr T. Tashiro (Cancer Chemotherapy Center, Japanese Foundation for Cancer Research, Tokyo, Japan). A piece of minced MX-1 tumor (2 x 2 mm) was inoculated subcutaneously into the right flank region of each mouse. The A549 human lung cancer cell line was obtained from the American Type Culture Collection (Rockville, Maryland, USA) and maintained in F-12K nutrient mixture supplemented with 10% (v/v) fetal bovine serum at 37°C under 5% CO_2. 5 x 10^6 cells of A549 were inoculated at the same site as the MX-1.

Antitumor agents

BV was obtained from F. Hoffman-La Roche Ltd. (Basle, Switzerland). Human IgG (HuIgG) was purchased from MP Biomedicals, Inc. (Solon, Ohio, USA). BV and HuIgG were diluted with saline. PTX was obtained from Wako Pure Chemical Industries (Osaka, Japan). PTX was dissolved in Cremophor EL-ethanol solution (1:1) and diluted 1:10 with saline just before administration. Cremophor EL-ethanol solution (1:1) diluted 1:10 with saline was administered as the PTX vehicle. Cremophor EL was purchased from Sigma-Aldrich Japan Co., Ltd. (Tokyo, Japan).

Evaluation of antitumor activity

After the tumors were sufficiently established in the mice, treatments with the antitumor agents were started (day 1). BV or HuIgG was administered intraperitoneally and PTX was administered intravenously once a week for 3 weeks for the evaluation of antitumor activity. The tumor volume was estimated by using the equation $V = ab^2/2$, in which a and b are the tumor length and width, respectively. Tumor volume was measured twice a week, and the degree of tumor growth inhibition was evaluated on day 22 (21 days after the initiation of the treatment).

Quantification of vascular permeability and MVD in tumors

Seventeen days after the MX-1 inoculation, BV or HuIgG at 5mg/kg and PTX at 30mg/kg were

administered once (day 1). Tumors were collected on day 2, day 5, and day 8. MVD and vascular permeability in the tumor were evaluated immunohistochemically. Immunohistochemical staining was performed using avidin–biotin–peroxidase complex on 5-μm thick sections from freshly frozen tissues. MVD (%) was calculated from the ratio of the CD31 stained area to the total area observed in three to six regions (0.4977mm^2 each). Vascular permeability in the tumor was determined from the difference between the area with CD31 positive staining and the area showing fluorescein isothiocyanate (FITC)–lectin positive staining in adjacent tissue sections (Hu *et al.*, 2005). FITC-labeled lectin (molecular weight 117K) was injected 1 h before collecting the tissues. Calculation of MVD and vascular permeability was performed automatically using the imaging analysis software Win ROOF (Mitani Corporation, Fukui, Japan). Rat anti-mouse CD31 monoclonal antibody clone MEC 13.3 (BD Biosciences, New Jersey, USA) and goat anti-FITC polyclonal antibody (Bethyl Laboratories, Inc., Texas, USA) were used in the assay. The MVD for each group was evaluated in four tumor samples.

Measurement of PTX concentration in plasma and tissue samples by HPLC

Sixteen days after the tumor inoculation, 30, 60, or 100 mg/kg of PTX was administered 1 h after the administration of 5mg/kg of BV or HuIgG in the MX-1 model. Mice were sacrificed 48 h after the PTX administration. Blood, tumor, and liver were collected. Plasma was obtained from the blood collected in a tube with sodium heparin by centrifugation at 10000 rpm for 10 min. Sixty microliters of plasma was mixed vigorously with 1 ml hexane–ethylacetate (1:1) in a reciprocal shaker for 30 min and then centrifuged at 2500 rpm for 10 min; 700 ml of the supernatant was evaporated to dryness. Tumor and liver were homogenized in a 19- or 4-fold volume of distilled water, respectively; 200 ml of the homogenate was mixed vigorously with 2 ml hexane–ethylacetate (1:1) in a reciprocal shaker for 30 min and then centrifuged at 2500 rpm for 10 min. Next, 1.5 ml of the supernatant was evaporated to dryness. The extraction residue was reconstituted in 500 ml of 90% acetonitrile solution, and aliquots of 35 ml were injected into a Lachrom D-7000 series high-performance liquid chromatography (HPLC) system consisting of a degasser (L-7610), pump (L-7100), programmable autosampler (L-7250), column oven (L-7300), and UV-vis detector (L-7420) (Hitachi High-Technologies Corporation, Tokyo, Japan). Chromatographic separation was achieved using a Capcell Pak UG120, S5, column (4.6 mm i.d. x 250 mm) with a Guard cartridge Capsell UG120, S5 (4.0 mm i.d. x 20 mm) (5 mm particle size, C18; Shiseido Company Limited, Tokyo, Japan). Elution was performed using a 15-min linear gradient from 40 to 95% (v/v) of acetonitrile. The mobile phase consisted of 95% acetonitrile held for 5 min, and then 40% acetonitrile held for 15 min. UV detection was performed at 227 nm. Ethanol, ethyl acetate, hexane, and acetonitrile were purchased from Wako Pure Chemical Industries. For pharmacokinetics

calculations, 30 mg/kg of PTX was administered 1 h after the administration of 5 mg/kg of HuIgG or BV in the MX-1 model. Mice were sacrificed 5 min, 1, 2, 4, 12, 18, 24, or 48 h after the PTX administration. Blood, tumor, and liver were treated and PTX concentration was measured by HPLC as described above. The mean concentration at each time point was used because of the nonserial blood sampling in this study. Pharmacokinetic parameters were calculated with the Watson software (Thermo Fisher Scientific Inc., Massachusetts, USA) using the model independent calculation method. The apparent terminal half-life ($T_{1/2}$) was calculated as 0.693/k.

Twenty-two days after the A549 tumor inoculation, 20 mg/kg of PTX was administered 1 h after the administration of 5 mg/kg of HuIgG or BV. Mice were sacrificed 48 h after the PTX administration. PTX concentration in the blood, tumor, and liver was analyzed by HPLC.

Statistical analysis

Statistical analysis for the evaluation of the antitumor activity and concentration of PTX was performed using the Wilcoxon test (SAS preclinical package, SAS Institute, Inc., Tokyo, Japan). Differences were considered to be significant at $P \leq 0.05$. A two-way analysis of variance was used to determine the differences in vascular permeability.

Results

Antitumor activity of BV as monotherapy and in combination therapy with PTX

I examined the antitumor activity of BV alone in an MX-1 human breast cancer xenograft model. BV at doses of 1.25, 5, or 20 mg/kg or HuIgG at 20 mg/kg as the control was administered. BV showed significant antitumor activity at doses of 5 and 20 mg/kg ($P \leq 0.05$, Fig. 10a). There was no significant decrease in body weight – an indicator of toxicity – during the treatment (Fig. 10b). The percentage of tumor growth inhibition after 3 weeks of administration of BV at 1.25, 5, or 20 mg/kg was 22, 64, and 61%, respectively. I also evaluated the antitumor activity of BV in combination with PTX in the same MX-1 tumor xenograft model. PTX and BV at the doses of 20 and 5 mg/kg, respectively, were administered once a week for 3 weeks. On day 22, there were statistically significant differences in tumor volume between the control and the groups treated with PTX, BV, and PTX-BV. Both PTX and BV significantly inhibited tumor growth (Fig. 11a). In the MX-1 model, tumor volume percent change against the control in the PTX and BV groups was 9.02 and 37.5%, respectively. Using these values to calculate percent change in the combination results in a change of 3.38%. However, in practice the tumor volume percent change in the combination group was 4.32%, and thus 7.70% lower than the calculated change. Hence, PTX and BV in combination showed potent activity, more than merely additive and with no reduction in body weight. There were no significant decreases in body weight on day 22 compared with day 1 in any of the groups (Fig. 11b). I also examined the antitumor activity of BV 5 mg/kg in combination with PTX 30 mg/kg. Tumor growth (Fig. 11c) was delayed because the potent efficacy of the combination resulted in tumor volume regression. The time required for tumor volume to reach 1000 mm^3 in the control, BV 5 mg/kg alone, PTX 30 mg/kg alone, and PTX-BV combination group was 11.3, 17.0, 53.1, and 84.9 days, respectively. The difference in time between BV alone and PTX-BV combination was 67.9 days, longer than that between the control group and PTX alone (41.8 days). The results indicate that BV inhibited tumor growth in combination with PTX.

Increase of PTX concentration in tumors by BV

To investigate the mechanism of the synergistic activity of PTX-BV combination therapy, I measured PTX concentration in the plasma, tumor and liver by HPLC (Fig. 12-14). PTX concentration of PTX-BV combination group in 48 h was significantly higher than that of PTX alone group (Fig. 13). I examined antitumor activity and PTX concentration in the groups. First, I compared the antitumor activity of PTX alone with that of the combination therapy of PTX-BV in the MX-1 model (Fig. 15a). Tumor volume in the groups treated with PTX alone at 10, 30, 60, and 100 mg/kg on day 22 showed dose-dependent tumor growth inhibition. The antitumor activity of 30

mg/kg PTX in combination with 5 mg/kg BV was comparable with that of PTX alone at both 60 and 100 mg/kg.

The concentration of PTX in the tumor in the mice treated with PTX 30 mg/kg plus BV 5 mg/kg was 5.75 ± 0.31 mg/g of tissue and was significantly higher than in the tumor treated with PTX 30mg/kg alone (4.00 ± 0.85 mg/g of tissue) 48 h after the PTX injection in the MX-1 model ($P = 0.0022$, Fig. 15b). The PTX concentration in the tumor treated with PTX 30 mg/kg plus BV 5 mg/kg was equivalent to that in the tumor treated with 100mg/kg of PTX. The PTX levels correspond to the degree of antitumor activity of PTX alone and PTX-BV. In contrast to the tumor, no remarkable differences were observed for PTX concentration in the plasma or liver between the PTX 30mg/kg plus BV 5mg/kg group and the PTX 30 mg/kg group. Maximum drug concentration (C_{max}) and $T_{1/2}$ values were calculated from the mean values of PTX concentration in each group (Table 2). The maximum drug concentration time (T_{max}) of PTX in the plasma, tumor, and liver were 5 min, 2 h and 5 min, respectively. After PTX injection, the PTX concentration was at the lower limit of quantification in the plasma at 12 h or later and in the liver at 18 h or later.

I also examined the effect of BV on PTX concentration in the human lung cancer xenograft model, A549, and again found an increase in PTX concentration, further showing the potent antitumor activity of the combination of PTX-BV (Fig. 16a). PTX concentrations in the tumor treated with PTX 20 mg/kg plus BV 5 mg/kg were significantly higher than those treated with PTX alone, as in the MX-1 model (Fig. 16b).

Decrease in the vascular permeability of tumors caused by BV

Next, I examined the decrease in the vascular permeability of the tumor caused by BV. A tumor treated with BV was collected on days 2, 5, and 8. The vascular permeability in the tumor was evaluated by the difference between the area with CD31-positive staining and the area with FITC–lectin-positive staining in adjacent tissue sections. Typical images from immunohistochemical staining and automated image processing using the analysis software Win ROOF are shown in Fig. 17. BV showed a significant decrease in the vascular permeability of tumor (Table 3). The ratio of the vascular permeability of the tumor treated with BV to the control tumor reached 50% by day 5.

Effect of BV or PTX-BV on MVD

I examined the effect of BV on MVD in the tumor of the MX-1 xenograft model by immunohistochemical staining for CD31. MVD on day 5 in the tumor of the BV alone group was significantly lower than in the control group (Fig. 18), but a further MVD decrease was not shown by the PTX-BV group. MVD in the PTX alone group also did not change significantly compared with that of the control group (data not shown).

Discussion

In a clinical study, BV in combination with PTX significantly prolonged progression-free survival and increased the objective response rate compared with PTX alone in patients with metastatic breast cancer (Miller *et al.*, 2007). In my present preclinical study, I also demonstrated the synergistic antitumor activity of BV in combination with PTX in a MX-1 breast cancer xenograft model and investigated the mechanism of this synergism.

Using the model, I examined tumor levels of PTX after treatment with this agent to investigate the effect of BV on tumors in combination chemotherapy. VEGF has been reported to increase vascular permeability and to elevate the IFP in tumors. Theoretically, the delivery rate of low-molecular-weight chemotherapeutic agents is reduced in tumors as a result of an increase in IFP and, as BV reduces the IFP, the delivery of the chemotherapeutic agents into the tumors is increased (Gerber and Ferrara, 2005). Indeed, Wildiers *et al*. (2003) has reported that A4.6.1 showed a tendency to increase the tumor level of CPT-11 in human colorectal cancer xenograft model. Dickson *et al*. (2007) also showed that BV induced increases in the tumor levels of topotecan and etoposide in human neuroblastoma xenograft models. In my study, BV treatment significantly increased the concentration of PTX in tumor compared with tumors treated with HuIgG. According to the elevation of PTX concentration in tumors, the degree of antitumor activity of PTX at 30 mg/kg administered in combination with BV was equivalent to that of 60 or 100 mg/kg alone. Therefore, in the MX-1 model, the synergistic antitumor activity of PTX-BV may be explained by the improved delivery of PTX into tumors.

The delivery of PTX into plasma or liver did not appear to be altered by BV administration. Therefore, VEGF produced by MX-1 tumor cells would affect the vascular permeability and the delivery of PTX into the tumors locally but not systemically. The following actions reported for BV may also be helpful in understanding the mechanism of synergism between BV and chemotherapeutic agents: blood vessel normalization (Jain, 2005), vascular permeability decrease (Gerber and Ferrara, 2005), and interstitial pressure decrease (Lee *et al.*, 2000; Willet *et al.*, 2004; Gerber and Ferrara, 2005). I investigated the change in vascular permeability in tumors as one of the parameters of blood vessel normalization by BV treatment and found that BV significantly decreased the permeability of the MX-1 tumors. This is the first report that demonstrates both increased PTX concentration and improved permeability in tumor by BV in a breast cancer xenograft model that also exhibits synergistic antitumor activity of BV in combination with PTX.

I attempted to measure the change in vascular flow by ultrasonic imaging and in IFP using the wick in needle technique (Fandes *et al.*, 1977) in the same MX-1 tumor. Unfortunately, at present, I have not established an appropriate evaluation system. No significant evidence was available

regarding causality between the decrease in vascular permeability and the increase in drug delivery. VEGF has been reported to block vessel maturation such as pericyte coverage (Verheul *et al.*, 2007; Lu *et al.*, 2008) and thus examination of vessel maturity is important in the investigation of vessel normalization by BV. However, in the present study, I did not explore vessel maturation to clarify the mechanism of PTX concentration increase in tumor because the increase in PTX concentration in tumor was recognized 49 h after BV treatment (48 h after PTX treatment), whereas I assume the time for vessel maturation is longer than 49 h. Further investigation into the mechanisms is needed to clarify the synergism.

Increase of PTX concentration can be caused by the decrease of vessel permeability in tumor vessels as described above. However, an alternative explanation is also possible for the PTX concentration increase, especially for the $T_{1/2}$ prolongation of PTX. This involves the lymphatic vessel. Although it has been considered that VEGFR-3 signaling contributes to the formation of the lymphatic vessel system, VEGF-A, VEGFR-2 and neuropilin have also been reported to function in lymphatic vessel formation (Cueni and Detmar, 2006). In consideration of the fact that BV binds to VEGF-A, it is possible that lymphatic vessel formation in tumor is further decreased and less PTX returns to vessels in the presence of BV. PTX has been shown to reduce MVD in tumors (Grant *et al.*, 2003). Therefore, I examined the possibility that PTX could reduce MVD and exert synergistic effects with the anti-angiogenic activity of BV. In the MX-1 model, however, PTX did not significantly reduce MVD in tumor and showed no significant augmentation of the anti-angiogenic activity of BV. These findings suggest that the mechanisms of the synergistic antitumor activity observed in the MX-1 model are not related to the additional reduction of MVD by the combination therapy.

In the present study, I demonstrated synergistic antitumor activity of BV with PTX in a breast cancer xenograft model. The improved delivery of PTX into the tumor helps to explain the mechanism of the synergistic effects of the combination of BV and PTX. Studies to further clarify the mechanism are needed.

General Discussion

It has long been recognized that construction of blood vessels in the tumors is necessary to supply sufficient nutrition and oxygen for tumor cells to proliferate. VEGF is an important factor in tumor angiogenesis and growth (Ferrara *et al.*, 1992; Ferrara and Davis-Smyth, 1997; Ferrara, 2004; Hoeben *et al.*, 2004). It is overexpressed in tumor cells compared to those in the normal tissues (Ferrara and Davis-Smyth, 1997; Hanrahan, 2003). Hypoxia in tumor triggers tumor cells to secrete VEGF which induces angiogenesis through signaling to the VEGFR in the blood vessels surrounding the tumor (Semenza, 2003; Ke and Costa, 2006). As to the cancer therapy, chemotherapeutic agents have been used for a long time. However, they cause severe side-effects because their activity is not specific to tumors. Thus, many molecular targeted agents, which are specific to molecular targets amplified or overexpressed in tumor cells, have been developed recently to limit toxicity and to improve the efficacy of cancer therapy, and are now used together with the conventional therapies. BV is the first molecular targeted agent for VEGF (Ferrara *et al.*, 2004) and is expected to suppress tumor growth by inhibiting angiogenesis via VEGF-VEGFR signaling.

In clinical studies, BV in combination with chemotherapeutic agents significantly prolonged progression-free survival and increased the objective response rate compared with chemotherapy alone in patients with CRC, NSCLC and BC (Hurwitz *et al.*, 2004; Kabbinavar *et al.*, 2003; Sandler *et al.*, 2006; Miller *et al.*, 2007). However, it is not clear why BV enhances the efficacy of the chemotherapeutic agents. To investigate the mechanisms of this synergistic effect of combination treatments, I established the animal models suitable in detecting antitumor activity of BV both as a monotherapy and as combination therapies with chemotherapeutic agents. BV alone showed significant antitumor activity in three human colorectal cancer xenograft models (COL-16-JCK, COLO 205, and CXF280). The MVD in tumors treated with BV was lower than that of the control on COL-16-JCK model. Antitumor activity of Cape-BV combination group was significantly higher than that of each agent alone (COL-16-JCK, COLO 205). Moreover, BV further enhanced the tumor suppressing activity of Cape-Oxali in COL-16-JCK xenograft model.

The synergistic effects of BV with chemotherapy have been attributed to the reduction in vascular permeability with normalization of the vasculature by obstructing the VEGF-VEGFR signaling. Vascular permeability reduction causes decrease of IFP and, consequently, chemotherapeutic agents are transferred abundantly to tumor cells in combination therapy of BV with chemotherapeutic agents (Jain, 2001; Gerber and Ferrara, 2005). The individual processes mentioned above have been fragmentally reported. For example, Wildiers *et al*. (2003) described that A4.6.1 showed a tendency to increase the tumor level of CPT-11 in human colorectal cancer

xenograft model. Dickson *et al*. (2007) also showed that BV induced increases in the tumor levels of topotecan and etoposide in human neuroblastoma xenograft models. Lee *et al*. (2000) has reported the reduced IFP in a xenograft model and Willet *et al*. (2004) showed the IFP decline 12 days after BV treatment in patients with rectal cancer. However, there is no report that verifies all of these processes.

In this study, taking the above hypothesis into account, I measured the PTX concentration in tumor and change of vascular permeability in the presence of BV in a MX-1 human breast cancer xenograft model to explain why BV showed synergistic antitumor activity with chemotherapeutic agents. BV treatment significantly increased the concentration of PTX in the tumor. Therefore, in the MX-1 model, the synergistic antitumor activity of PTX-BV may be explained by the improved delivery of PTX into tumors. In addition, BV significantly decreased the vascular permeability of the MX-1 tumors. These results support the idea that BV inhibition of VEGF-VEGFR signaling results in vascular permeability reduction and cause the IFP decrease in tumor, which in turn contributes to an increase of PTX concentration in tumors (Fig. 19). The only unverified point is the IFP change followed by permeability reduction. This is an issue to be solved in the future. Since VEGF has been reported to block vessel maturation such as pericyte coverage (Verheul *et al.*, 2007, Lu *et al.*, 2008), examination of vessel maturity is also important in the investigation of vessel normalization by BV. Currently, it is not clear whether the vessel maturity is correlated with permeability in tumor. Evaluation of pericyte coverage by BV is another important issue to comprehend the role of VEGF-VEGFR signaling.

It should be noted that there is an alternative explanation for the PTX concentration increase: the $T_{1/2}$ prolongation of PTX. It is considered the possibility of MVD and lymphangiogenesis inhibition by BV and decline of the PTX recovery from tumors to microvessel or lymphatic vessel. Although it is generally accepted that VEGFR-3 causes the formation of the lymphatic vessel system (Karkkainen *et al.*, 2002), there is a report that VEGF-A, VEGFR-2 and neuropilin also function in lymphatic vessel formation (Cueni and Detmar, 2006). VEGF-A potency induces proliferation of lymphangiogenesis *in vitro* (Hirakawa *et al*., 2003), and injection of adenoviral murine VEGF-A_{164} resulted in pronounced and persistent *in vivo* lymphangiogenesis in mouse ear skin (Nagy *et al*., 2002). Targeted overexpression of murine VEGF-A_{164} in the skin of transgenic mice enhanced lymphangiogenesis as well as angiogenesis during tissue repair and in skin inflammation (Kunstfeld *et al*., 2004; Hong *et al*., 2004). Since BV binds to VEGF-A, lymphatic vessel formation in tumor can be further decreased by BV so that less PTX returns to vessels. This possibility awaits further investigation.

The timing of BV treatment is also a matter of consideration. In my study, BV was administered just 1 h prior to PTX administration, expecting the immediate improvement of the vessel

permeability. Dickson *et al*. administered chemotherapeutic agents much later (Dickson *et al*., 2007). They injected topotecan or etoposide to mice 1, 3 and 7 days after the BV administration. The topotecan concentration of the combination group with BV was significantly higher than that of topotecan alone group, when topotecan was administered 3 days after BV treatment. However, this elevation was no longer seen on day 7. Meanwhile, etoposide concentration in tumor was elevated on day 1. However, this improvement had already declined on day 3. Thus, the tumor concentration of medicine was changed depending on the length of prior BV treatment and on the physicochemical properties of the medicine as well. Indeed, the greatest difference of permeability between control group and BV treatment group was observed on day 5 in my study. Further investigation is needed to clear the mechanism of improvement of permeability and tumor concentration of medicine.

Currently, ten antibody medicines, including BV which neutralizes VEGF, are available to treat hematological cancer or solid tumor. Generally, two or three anticancer medicines, including low molecular agents and antibody medicines, have been used in combination to treat solid tumor. It is important to make clear the rationale, why the combination therapy is more effective than the monotherapy, not only because I can explain it to patients and doctors but also the knowledge will contribute to revealing biological characteristics of the tumor and to further advancements in antitumor therapy. This study shows the rationale of BV and PTX combination therapy. Discovering the timing of BV administration at which other anticancer agents are maximally concentrated in tumor may make it possible to propose a new effective modality of BV combination therapy. Furthermore, clarifying the mechanism by which permeability in tumor tissue is improved would make the role of VEGF clearer.

The essential parts of this thesis have been published in the major journals on anticancer chemotherapeutic studies (Yanagisawa *et al.*, 2009; Yanagisawa *et al.*, 2010).

Acknowledgements

I would like to thank Professor Hideko Urushihara, University of Tsukuba, for her valuable advice and encouragement every time throughout preparing this dissertation.

I wish to thank Associate Professor Kouji Nakamura, University of Tsukuba, for his kindly support to take my doctor program. I also sincerely thank Dr. Keiji Saito, Chugai Academy for Advanced Oncology, for recommending me to take a degree and encouragement. I also thank Dr. Kazuo Nakamura, Chugai Pharmaceutical Co. Ltd., for his special support for my doctor program and encouragement.

I sincerely thank Dr. Kazushige Mori and Dr. Kaori Ouchi for their suggestions and instructions regarding many experiments and discussions. I also thank Dr. Keigo Yorozu and Ms. Mitsue Kurasawa for immunohistochemical studies. I also thank Mr. Haruyoshi Shirai for operating high-performance liquid chromatography and his helpful advice, and Dr. Kohnosuke Nakano for analysis of pharmacokinetics. I also thank Mr. Koh Furugaki for animal experiments and Ms. Yoriko Yamashita for biological assays. Many thanks also to all the members of my laboratory for their support.

References

Akiyama S, Furukawa T, Sumizawa T, Takebayashi Y, Nakajima Y, Shimaoka S, Haraguchi M. The role of thymidine phosphorylase, an angiogenic enzyme, in tumor progression. Cancer Sci 2004; 95: 851-857.

Achen MG, Jeltsch M, Kukk E, Mäkinen T, Vitali A, Wilks AF, Alitalo K, Stacker SA. Vascular endothelial growth factor D (VEGF-D) is a ligand for the tyrosine kinases VEGF receptor 2 (Flk1) and VEGF receptor 3 (Flt4). Proc Natl Acad Sci USA 1998; 95: 548–553.

Carmeliet P. Angiogenesis in health and desease. Nat Med 2003; 9: 653-660.

Connolly DT, Olander JV, Heuvelman D, Nelson R, Monsell R, Siegel N, Haymore BL, Leimgruber R, Feder J. Human vascular permeability factor: Isolation from U937 cells. J Biol Chem 1989; 264: 20017-20024.

Cueni LN, Detmar M. New insights into molecular control of the lymphatic vascular system and its role in disease. J Invest Dermat 2006; 126: 2167-2177.

Dai J, Rabie ABM. VEGF: an essential mediator of both angiogenesis and endochondral ossification. J Dent Res 2007; 86: 937-950.

Dickson PV, Hamner JB, Sims TL, Fraga CH, Ng CYC, Rajasekeran S, Hagedorn NL, McCarville MB, Clinton F. Stewart CF, Davidoff AM. Bevacizumab-induced transient remodeling of the vasculature in neuroblastoma xenografts results in improved delivery and efficacy of systemically administered chemotherapy. Clin Cancer Res 2007; 13: 3942-3950.

Ehrmann RL, Knoth M. Choriocarcinoma: Transfilter stimulation of vasoproliferation in the hamster cheek pouch-Studied by light and electron microscopy. J Natl Cancer Inst 1968; 41: 1329-1341.

Endo M, Shinbori N, Fukase Y, Sawada N, Ishikawa T, Ishitsuka T, Tanaka Y. Induction of thymidine phosphorylase expression and enhancement of efficacy of capecitabine or 5'-deoxy-5-fluorouridine by cyclophosphamide in mammary tumor models. Int J Cancer 1999; 83: 127-134.

Fandes HO, Reed RK, Aukland K. Interstitial fluid pressure in rats measured with a modified wick technique. Microvasc Res 1977; 14: 27-36.

Ferrara N, Henzel WJ. Pituitary follicular cells secrete a novel heparin-binding growth factor specific for vascular endotherial cells. Biochem Biophys Res Commun 1989; 161: 851-858.

Ferrara N, Houck K, Jakeman L, Leung DW. Molecular and biological properties of the vascular endothelial growth factor family of proteins. Endocr Rev 1992; 13: 18-32.

Ferrara N, Davis-Smyth T. The biology of vascular endothelial growth factor. Endocr Rev 1997; 18: 4-25.

Ferrara N. Vascular endothelial growth factor: basic science and clinical progress. Endocr Rev 2004; 25: 581-611.

Ferrara N, Hillan KJ, Gerber H-P, Novotny W. Discovery and development of bevacizumab, an anti-VEGF antibody for treating cancer. Nat Rev Drug Discov 2004; 3: 391-400.

Folkman J. Tumor angiogenesis: Therapeutic implications. N Engl J Med 1971; 285: 1182-1186.

Folkman J, Merler E, Abernathy C, Williams G. Isolation of a tumor factor responsible for angiogenesis. J Exp Med 1971; 133: 275-288.

Folkman J, Klagsbrun M. Angiogenic factors. Science 1987; 235: 442-447.

Folkman J. What is the evidence that tumors are angiogenesis dependent? J Natl Cancer Inst. 1990; 82: 4-6.

Garlanda C, Berthier R, Garin J, Stoppacciaro A, Ruco L, Vittet D, Gulino D, Matteucci C, Mantovani A, Vecchi A, Dejana E. Characterization of MEC 14.7, a new monoclonal antibody recognizing mouse CD34: a useful reagent for identifying and characterizing blood vessels and hematopoietic precursors. Eur J Cell Biol 1997; 73: 368-377.

Gerber H-P, Ferrara N. Pharmacology and pharmacodynamics of bevacizumab as monotherapy or in combination with cytotoxic therapy in preclinical studies. Cancer Res 2005; 65: 671-680.

Grant DS, Williams TL, Zahaczewsky M, Dicker AP. Comparison of antiangiogenic activities using paclitaxel (Taxol) and docetaxel (Taxotre). Int. J. Cancer 2003; 104: 121‑129.

Greenblatt M, Shubick P. Tumor angiogenesis: transfilter diffusion studies in the hamster by the transparent chamber technique. J Natl Cancer Inst 1968; 41: 111-124.

Hanrahan V, Currie MJ, Gunningham SP, Morrin HR, Scott PAE, Robinson BA, Fox SB. The angiogenic switch for vascular endothelial growth factor (VEGF)-A, VEGF-B, VEGF-C, and VEGF-D in the adenoma–carcinoma sequence during colorectal cancer progression. J Pathol 2003; 200: 183–194.

Hashizume H, Baluk P, Morikawa S, McLean JW, Thurston G, Roberg S, Jain RK, McDonald DM. Openings between defective endothelial cells explain tumor vessel leakiness. Am J Pathol 2000; 156: 1363-1380.

Hirakawa S, Hong YK, Harvey N, Schacht V, Matusda K, Libermann T, Detmar M. Identification of vascular lineage-specific genes by transcriptional profiling of isolated blood vascular and lymphatic endothelial cells. Am J Pathol 2003; 162: 575-586.

Hoeben A, Landuyt B, Highley MS, Wildiers H, van Oosterom AT, de Bruijn EA. Vascular endothelial growth factor and angiogenesis. Pharmcol Rev 2004; 56: 549-580.

Hong YK, Lange-Asschenfeldt B, Velasco P, Hirakawa S, Kunstfeld R, Brown LF, Bohlen P, Senger DR, Detmar M. VEGF-A promotes tissue repair-associated lymphatic vessel formation via VEGFR-2 and the α1β1 and α2β1 integrins. FASEB J 2004; 18: 1111-1113.

Horwitz SB. Mechanism of action of taxol. Trends Pharmacol Sci 1992; 13: 134-136.

Houck KA, Ferrara N, Winer J, Cachianes G, Li B, Leung DW. The vascular endothelial growth factor family: identification of a fourth molecular species and characterization of alternative splicing of RNA. Mol Endocrinol. 1991; 5:1806-1814.

Hu L, Hofmann J, Jaffe RB. Phosphatidylinositol 3-kinase mediates angiogenesis and vascular permeability associated with ovarian carcinoma. Clin Cancer Res 2005; 11: 8208-8212.

Hurwitz H, Fehrenbacher L, Novotny W, Cartwright T, Hainsworth J, Heim W, Berlin J, Baron A, Griffing S, Holmgren E, Ferrara N, Fyfe G, Rogers B, Ross R, Kabbinavar F. Bevacizumab plus irinotecan, fluorouracil and leucovorin for metastatic colorectal cancer. N Engl J Med 2004; 350: 2335-2342.

Ide AG, Baker NH, Warren SL. Vascularization of the brown-pearce rabbit epithelioma transplant as seen in the transparent ear chamber. Am J Roentgenol 1939; 42: 891-899.

Ishikawa T, Sekiguchi F, Fukase Y, Sawada N, Ishituka H. Positive correlation between the efficacy of capecitabine and doxifluridine and the ratio of thymidine phosphorylase to dihydropyrimidine dehydrogenase activities in tumors in human cancer xenografts. Cancer Res 1998; 58: 685-690.

Ishituka H, Ishikawa T, Fukase Y, Sawada N, Tanaka Y, Ouchi K, Yshokubo T, Nishida M. Capecitabine and the dThdPase up-regulators IFNγ or Taxol showed synergistic activity in human cancer xenografts. Proc Am Assoc Cancer Res 1996; 37: 405.

Jain RK. Normalizing tumor vasculature with anti-angiogenic therapy: a new paradigm for combination therapy. Nat Med 2001; 7: 987–989.

Jain RK. Molecular regulation of vessel maturation. Nat Med 2003; 9: 685-693.

Jain RK. Normalization of tumor vasculature: an emerging concept in antiangiogenic therapy. Science 2005; 307: 58–62.

Joukov V, Pajusola K, Kaipainen A, Chilov D, Lahtinen I, Kukk E, Saksela O, Kalkkinen N, Alitalo K. A novel vascular endothelial growth factor, VEGF-C, is a ligand for the Flt4 (VEGFR-3) and KDR (VEGFR-2) receptor tyrosine kinases. EMBO J 1996; 15: 290-298.

Kabbinavar F, Hurwitz HI, Fehrenbacher L, Meropol NJ, Novotny WF, Lieberman G, Griffing S, Bergsland E. Phase II, randomized trial comparing bevacizumab plus fluorouracil (FU)/leucovorin (LV) with FU/LV alone in patients with metastatic colorectal cancer. J Clin Oncol 2003; 21: 60-65.

Karkkainen MJ, Mäkinen T, Alitalo K. Lymphatic endothelium: a new frontier of metastasis

research. Nat Cell Biol 2002; 4: E2–E5.

Ke Q, Costa M. Hypoxia-inducible factor-1 (HIF-1). Mol Pharmacol 2006; 70:1469-1480.

Kim KJ, Li B, Houck K, Winer J, Ferrara N. The vascular endothelial growth factor proteins: identification of biologically relevant regions by neutralizing monoclonal antibodies. Growth Factors 1992; 7: 53-64.

Kim KJ, Li B, Winer J, Armanini M, Gillett N, Phillips HS, Ferrara N. Inhibition of vascular endothelial growth factor-induced angiogenesis suppresses tumor growth in vivo. Nature. 1993; 362: 841-844.

Klagsbrun M, Knighton D, Folkman J. Tumor angiogenesis activity in cells grown in tissue culture. Cancer Res 1976; 36: 110-114.

Kunstfeld R, Hirakawa S, Hong YK, Schacht V, Lange-Asschenfeldt B, Velasco P, Lin C, Fiebiger E, Wei X, Wu Y, Hicklin D, Bohlen P, Detmar M. Induction of cutaneous delayed-type hypersensitivity reactions in VEGF-A transgenic mice results in chronic skin inflammation associated with persistent lymphatic hyperplasia. Blood 2004; 104: 1048-1057.

Lee CG, Heijn M, di Tomaso E, Griffon-Etienne G, Ancukiewicz M, Koike C, Park KR, Ferrara N, Jain RK, Suit HD, Boucher Y. Anti-vascular endothelial growth factor treatment augments tumor radiation response under normoxic or hypoxic conditions. Cancer Res. 2000; 60: 5565-5570.

Leung DW, Cachianes G, Kuang W-J, Goeddel DV, Ferrara N. Vascular endothelial growth factor is a secreted angiogenic mitogen. Science 1989; 246: 1306-1309.

Lu C, Thaker PH, Lin Yvonne G, Spannuth W, Landen CN, Merritt WM, Jennings NB, Langley RR, Gershenson DM, Yancopoulos GD, Ellis LM, Jaffe RB, Coleman RL, Sood AK. Impact of vessel maturation on antiangiogenic therapy in ovarian cancer. Am J Obstet Gynecol 2008; 198: 477.e1-477.e10.

Martinelli E, De Palma R, Orditura M, De Vita F, Ciardiello F. Anti-epidermal growth factor receptor monoclonal antibodies in cancer therapy. Clin Exp Immunol 2009; 158: 1-9.

Mass RD. The HER receptor family: a rich target for therapeutic development. Int. J Radiat Oncol Biol Phys 2004; 58: 932-940.

McDonald DM, Choyke PL. Imaging of angiogenesis: from microscopic to clinic. Nat Md 2003; 9: 713-725.

Miller K, Wang M, Gralow J, Dickler M, Cobleigh M, Perez EA, Shenkier T, Cella D, Davidson NE. Paclitaxel plus bevacizumab versus paclitaxel alone for metastatic breast cancer. N Engl J Med 2007; 357: 2666-2676.

Müller YA, Chen Y, Christinger HW, Li B, Cunningham BC, Lowman HB, de Vos AM. VEGF and

the Fab fragment of a humanized neutralizing antibody: crystal structure of the complex at 2.4 A resolution and mutational analysis of the interface. Structure 1998; 6: 1153-1167.

Nagy JA, Vasile E, Feng D, Sundberg C, Brown LF, Detmar MJ, Lawitts JA, Benjamin L, Tan X, Manseau EJ, Dvorak AM, Dvorak HF. Vascular permeability factor/vascular endothelial growth factor induces lymphangiogenesis as well as angiogenesis. J Exp Med 2002; 196: 1497-1506.

Nishida M, Hino A, Mori K. Matsumoto T, Yoshikubo T, Ishitsuka H. Preparation of anti-human thymidine phosphorylase monoclonal antibodies useful for detecting the enzyme levels in tumor tissues. Biol Pharm Bull 1996; 19: 1407-1411.

Normanno N, Bianco C, De Luca A, Maiello MR, Salomon DS. Target-based agents against ErbB receptors and their ligands: a novel approach to cancer treatment. Endocr Relat Cancer 2003; 10: 1-21.

Normanno N, Morabito A, De Luca A, Piccirillo MC, Gallo M, Maiello MR, Perrone F. Target-based therapies in breast cancer: current status and future perspectives. Endocr Relat Cancer 2009; 16: 675-702.

Ogawa S, Oku A, Sawano A, Yamaguchi S, Yazaki Y, Shibuya M. A novel type of vascular endothelial growth factor, VEGF-E (NZ-7 VEGF), preferentially utilizes KDR/Flk-1 receptor and carries a potent mitotic activity without heparin-binding domain. J Biol Chem 1998; 273: 31273–31282.

Olofsson B, Pajusola K, Kaipainen A, von Euler G, Joukov V, Saksela O, Orpana A, Pettersson RF, Alitalo K, Eriksson U. Vascular endothelial growth factor B, a novel growth factor for endothelial cells. Proc Natl Acad Sci USA 1996; 93: 2576–2581.

Otrock ZK, Makarem JA, Shamseddine AI. Vascular endothelial growth factor family of ligands and receptors: Review. Blood Cells Mol Dis 2007; 38: 258-268.

Pérez-Soler R. HER1/EGFR targeting: Refining the strategy. Oncologist 2004; 9: 58-67

Presta LG, Chen H, O'Connor SJ, Chishlm V, Meng YG, Krummen L, Winkler M, Ferrara1 N. Humanization of an anti-vascular endothelial growth factor monoclonal antibody for the therapy of solid tumors and other disorders. Cancer Res 1997; 57: 4593-4599.

Ronellenfitsch MW, Steinbach JP, Wick W. Epidermal growth factor receptor and mammalian target of rapamycin as therapeutic targets in malignant glioma: current clinical status and perspectives. Targ Oncol 2010; 5: 183-191.

Rydberg B. Radiation-induced DNA damage and chromatin structure. Acta Oncologica 2001; 40: 682–685.

Saltz LB, Clarke S, Díaz-Rubio E, Scheithauer W, Figer A, Wong R, Koski S, Lichinister M, Yang T-S, Rivera F, Couture F, Sirzén F, Cassidy J. Bevacizumab in combination with oxaliplatin-based chemotherapy as first-line therapy in metastatic colorectal cancer: a randomized phase III study. J

Clin Oncol 2008; 26: 2013-2019.

Sandison JC. Observations on growth of blood vessels as seen in transparent chamber introduced into rabbit's ear. Am J Anat 1928; 41: 475-496.

Sandler A, Gray R, Perry MC, Brahmer J, Schiller JH, Dowlati A, Lilenbaum R, Johnson DH. Paclitaxel-carboplatin alone or with bevacizumab for non-small-cell lung cancer. N Engl J Med 2006; 355: 2542-2550.

Sawada N, Ishikawa T, Fukase Y, Nishida M, Yoshikubo T, Ishituka H. Induction of thymidine phosphorylase activity and enhancement of capecitabine efficacy by Taxol/Taxotere in human cancer xenografts. Clin Cancer Res 1998; 4: 1013-1019.

Sawada N, Kondoh K, Mori K. Enhancement of capecitabine efficacy by oxaliplatin in human colorectal and gastric cancer xenografts. Oncol Rep 2007; 18: 775-778.

Semenza GL. Targeting HIF-1 for cancer therapy. Nat Rev Cancer 2003; 3: 721-732.

Sengar DR, Galli SJ, Dvorak AM, Perruzzi CA, Harvey VS, Dvorak HF. Tumor cells secrete a vascular permeability factor that promotes accumulation of ascites fluid. Science 1983; 219: 983-985.

Shibuya M, Claesson-Welsh L. Signal transduction by VEGF receptors in regulation of angiogenesis and lymphangiogenesis. Exp Cell Res 2006; 312: 549-560.

Suto K, Yamazaki Y, Morita T, Mizuno H. Crystal structures of novel vascular endothelial growth factors (VEGF) from snake venoms: Insight into selective VEGF binding to kinase insert domain-containing receptor but not to fms-like tyrosine kinase-1. J Biol Chem 2005; 280: 2126-2131.

Tischer E, Mitchell R, Hartman T, Silva M, Gospodarowicz D, Fiddes JC, Abraham JA. The human gene for vascular endothelial growth factor: Multiple protein forms are encoded through alternative exon splicing. J Biol Chem 1991; 266: 11947-11954.

Verheul HMW, Hammers H, van Erp K, Wei Y, Sanni T, Salumbides B, Qian DZ, Yancopoulos GD, Pili R. Vascular endotherial growth factor trap blocks tumor growth, metastasis formation, and vascular leakage in an orthotropic murine renal cell cancer model. Clin Cancer Res 2007; 13: 4201-4208.

Wang Y, Fei D, Vanderlaan M, Song A. Biological activity of bevacizumab, a humanized anti-VEGF antibody, in vitro. Angiogenesis 2004; 7: 335-345.

Warren RS, Yuan H, Matli MR, Gillett NA, Ferrara N. Regulation by vascular endothelial growth factor of human colon cancer tumorigenesis in a mouse model of experiemental liver metastasis. J Cin Invest. 1995; 95: 1789-1797.

Wildiers H, Guetens G, De Boeck G, Verbeken E, Landuyt B, Landuyt W, de Bruijn EA, van

Oosterom AT. Effect of antivascular endothelial growth factor treatment on the intratumoral uptake of CPT-11. Br J Cancer 2003; 88: 1979-1986.

Willet CG, Boucher Y, di Tomaso E, Duda DG, Munn LL, Tong RT, Chung DC, Sahani DV, Kalva SP, Kozin SV, Mino M, Cohen KS, Scadden DT, Hartford AC, Fischman AJ, Clark JW, Ryan DP, Zhu AX, Blaszkowsky LS, Chen HX, Shellito PC, Lauwers GY, Jain RK. Direct evidence that the VEGF-specific antibody bevacizumab has antivascular effects in human rectal cancer. Nat Med 2004; 10: 145-147.

Yanagisawa M, Fujimoto-Ouchi K, Yorozu K, Yamashita Y, Mori K. Antitumor activity of bevacizumab in combination with capecitabine and oxaliplatin in human colorectal cancer xenograft models. Oncol Rep 2009; 22: 241-247.

Yanagisawa M, Yorozu K, Kurasawa M, Nakano K, Furugaki K, Yamashita Y, Mori K, Fujimoto-Ouchi K. Bevacizumab improves the delivery and efficacy of paclitaxel. Anticancer drugs 2010; 21: 687-694.

Tables

Table 1. Levels of TP from treatment with BV and VEGF from treatment with Cape in COL-16-JCK and COLO 205 xenografts.

Cell line	TP level (unit/mg protein)		VEGF level (pg/mg protein)	
	HuIgG (4 mg/kg)	BV (4 mg/kg)	Vehicle	Cape (539 mg/kg)
COL-16-JCK	2.1 ± 0.7	2.7 ± 5.8	281.2 ± 36.0	272.0 ± 21.3
COLO 205	8.5 ± 0.6	9.5 ± 2.4	NT	NT

HuIgG or BV was administered i.p. twice a week for 3 weeks. Cape was given p.o. daily for 13 days. The levels of TP and VEGF in tumor were measured by ELISA. NT: not tested.

Table 2. C_{max} and $T_{1/2}$ of PTX in PTX alone or PTX-BV groups in a MX-1 xenograft model.

	C_{max} (μg/ml)	C_{max} (μg/g tissue)		$T_{1/2}$ (h)		
Administration	Plasma	Tumor	Liver	Plasma	Tumor	Liver
PTX 30 mg/kg + HuIgG 5 mg/kg	60.4	12.9	201	0.952	39.0	1.66
PTX 30 mg/kg + BV 5 mg/kg	70.0	12.9	226	0.834	68.6	1.46
Δ%	16%	0%	12%	-12%	76%	-12%

PTX was administered intravenously 1 h after HuIgG or BV was administered intraperitoneally. Mice were sacrificed within 5min to 48 h after the administration of PTX. Blood, tumor, and liver were collected from each mouse and PTX concentration was analyzed by high-performance liquid chromatography. C_{max} or $T_{1/2}$ was calculated from the average of each group (n = 6/group).

Table 3. Effect of BV on vascular permeability in MX-1 tumor

	Permeability (%)			
Administration	Day 2	Day 5	Day 8	p value
Control (HuIgG 5 mg/kg)	3.05 ± 1.65	3.65 ± 1.37	2.87 ± 1.24	-
BV 5 mg/kg	2.25 ± 1.05	1.80 ± 1.18	1.80 ± 0.94	0.0315

Statistical analysis of the difference between the control and the BV group was performed using a two-way analysis of variance.

Figures

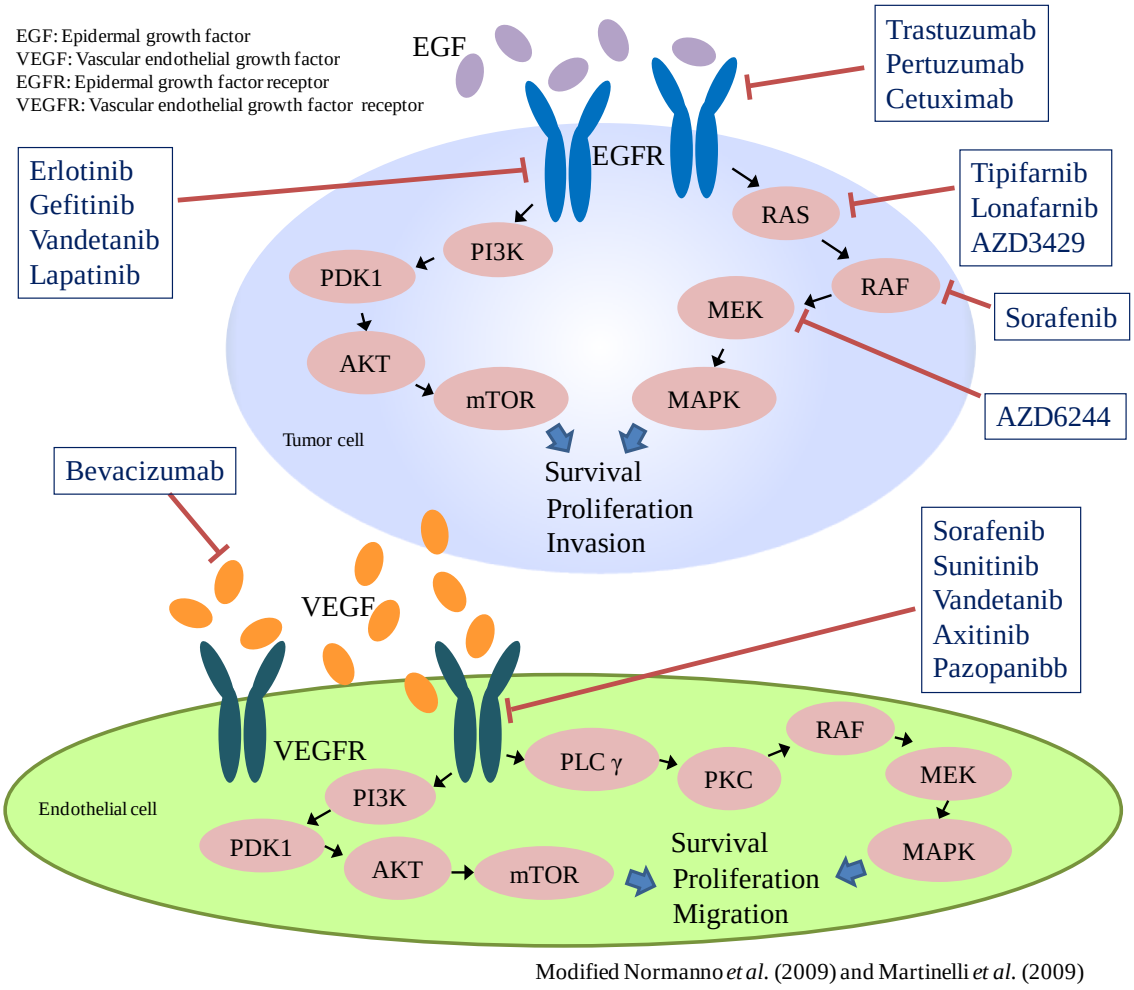

Modified Normanno *et al.* (2009) and Martinelli *et al.* (2009)

Figure 1. Growth factor signal pathways and molecular targeted agents. Binding of specific ligands that are produced by either tumor cells or by surrounding stromal cells activate growth factor receptors. The activated receptors transfer the signals and cause survival, proliferation and invasion of tumor cells. VEGF, which is secreted by tumor cells, binds VEGFR. VEGFR leads to the activation of intracellular signaling transduction pathways that involves endothelial cell proliferation, migration and survival.

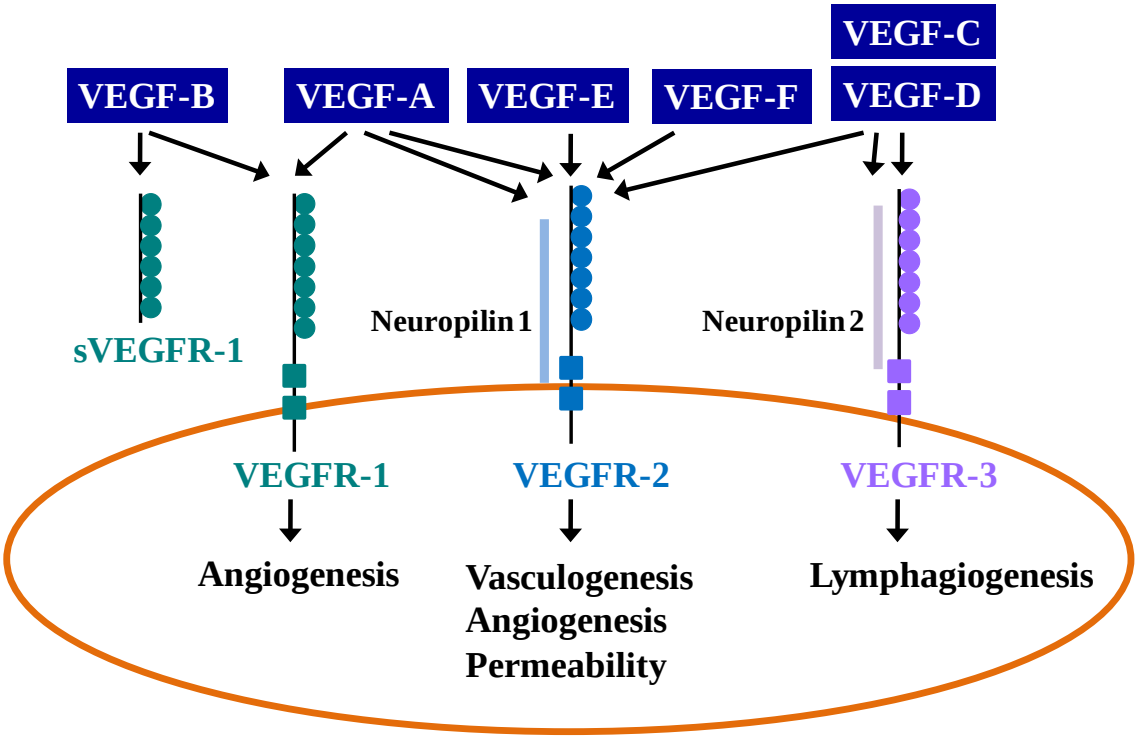

Figure 2. Outputs of VEGF-VEGFR signaling. VEGF is a glycoprotein with a molecular weight of 45,000. Six subtypes of VEGF (VEGF-A, -B, -C, -D, -E and -F) and three receptors (VEGFR-1, -2 and -3) are known. Each VEGF subtype binds to multiple VEGFR. Activation of VEGFR-1 results in angiogenesis and migration of hematopoietic cells, of VEGFR-2, vasculogenesis, angiogenesis, permeability and of VEGFR-3, lymphatic formation.

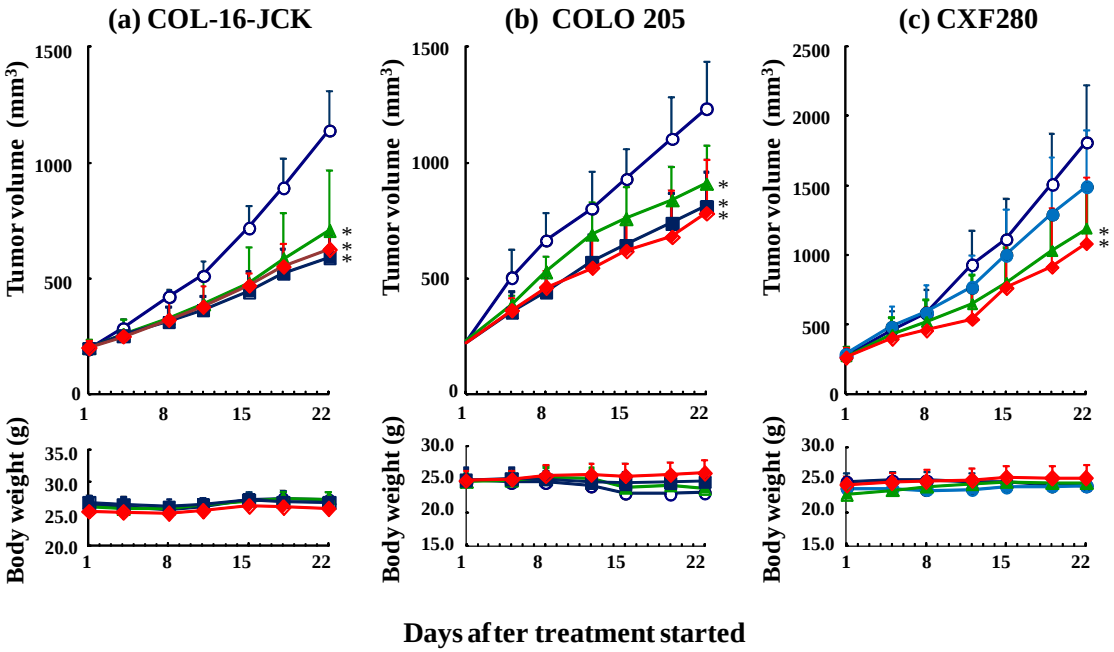

Figure 3. Antitumor activity of BV in COL-16-JCK (a), COLO 205 (b) and CXF280 (c) human colorectal cancer xenograft models. Mice were randomly divided into 4 groups (n = 5 or 6/group). HuIgG or BV was administered i.p. twice a week for 3 weeks. Data points indicate mean values + SD of tumor volume or body weight. ○, HuIgG 4.0 mg/kg (control group); ●, BV 0.4 mg/kg; ▲, BV 1.2 mg/kg; ■, BV 2.5 mg/kg; ◆, BV 4.0 mg/kg. *P < 0.05 vs. control group.

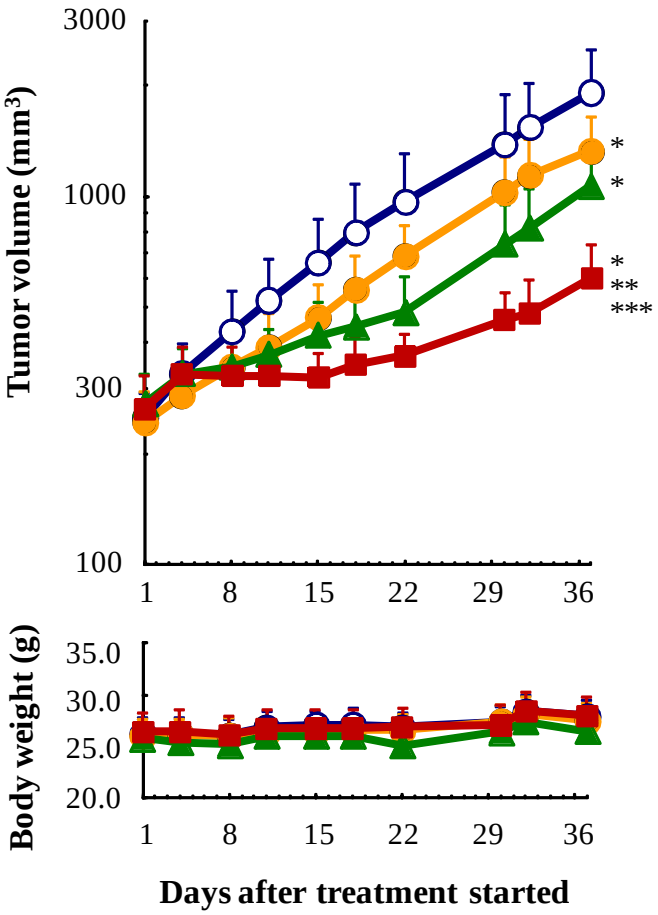

Figure 4. Antitumor activity of BV in combination with Cape in COL-16-JCK human colorectal cancer xenograft models. HuIgG or BV was administered i.p. twice a week for 3 weeks and Cape was given p.o. daily for 14 days. Data points indicate mean values + SD of tumor volume or body weight (n = 6). ○, HuIgG 4 mg/kg (control group); ●, BV 4 mg/kg; ▲, Cape 359 mg/kg; ■, Cape 359 mg/kg and BV 4 mg/kg. $^{*}P < 0.05$ vs. control group; $^{**}P < 0.05$ vs. Cape group; $^{***}P < 0.05$ vs. BV group.

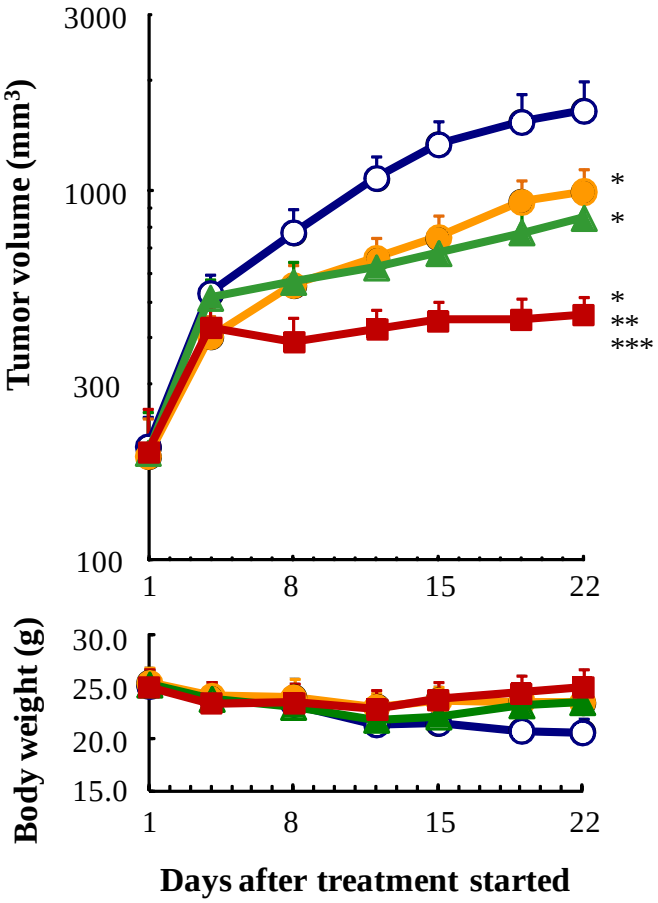

Figure 5. Antitumor activity of BV in combination with Cape in COLO 205 human colorectal cancer xenograft models. HuIgG or BV was administered i.p. twice a week for 3 weeks and Cape was given p.o. daily for 14 days. Data points indicate mean values + SD of tumor volume or body weight (n = 6). ○, HuIgG 4 mg/kg (control group); ●, BV 4 mg/kg; ▲, Cape 269 mg/kg; ■, Cape 269 mg/kg and BV 4 mg/kg. $^{*}P < 0.05$ vs. control group; $^{**}P < 0.05$ vs. Cape group; $^{***}P < 0.05$ vs. BV group.

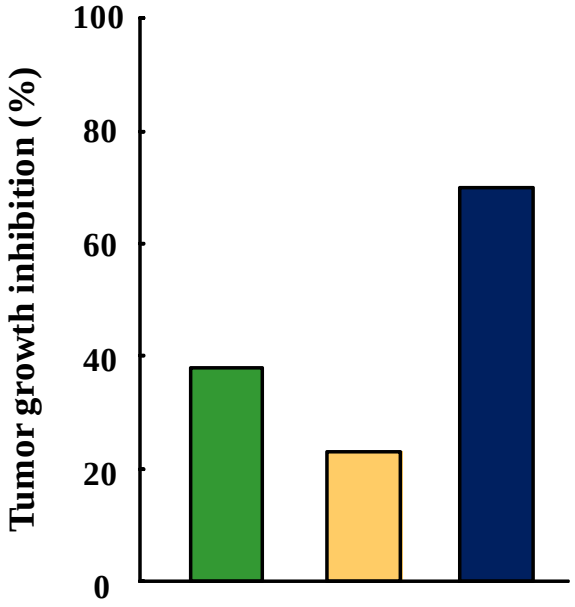

Figure 6. Tumor growth inhibition (%) of Cape-Oxali in COL-16-JCK. Mice were randomly divided into groups (n = 6). Cape (180 mg/kg) was administered p.o. once a day for 14 days. Five mg/kg of Oxali was administered i.v. on Day 1. TGI was evaluated on Day 36.Tumor growth inhibition (%) of Cape-Oxali in COL-16-JCK. Mice were randomly divided into groups (n = 6). 180 mg/kg of Cape was administered p.o. once a day for 14 days. 5 mg/kg of Oxali was administered i.v. on Day 1. TGI was evaluated on Day 36.

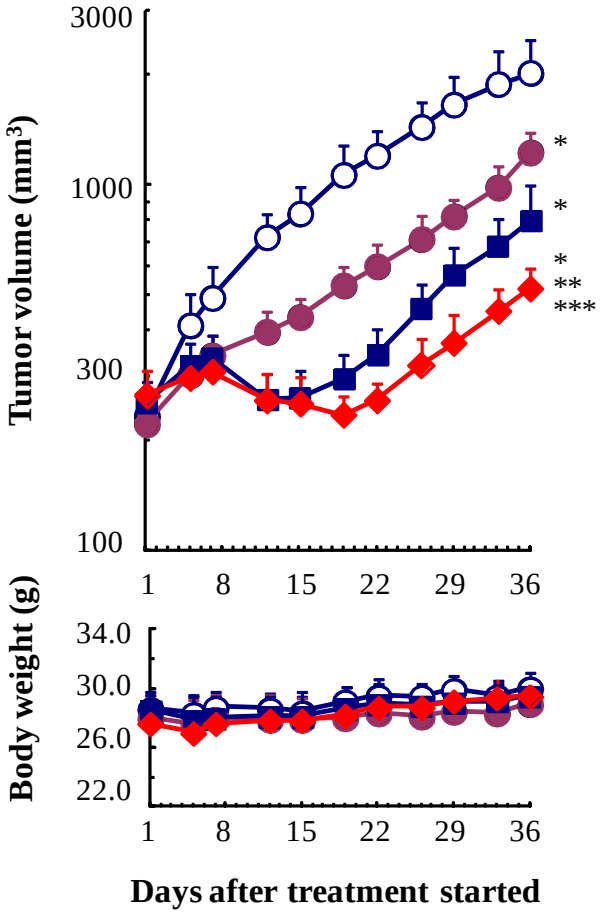

Figure 7. Antitumor activity of BV in combination with Cape-Oxali in COL-16-JCK. HuIgG or BV was administered i.p. twice a week for 3 weeks and Cape was given p.o. daily for 14 days. Oxali was administered i.v. on Day 1. Data points indicate mean values + SD of tumor volume or body weight (n = 6). ○, HuIgG 4 mg/kg (control group); ●, BV 4 mg/kg; ■, Cape 180 mg/kg and Oxali 5 mg/kg (Cape-Oxali); ◆, Cape 180 mg/kg, Oxali 5 mg/kg, and BV 4 mg/kg. $^{*}P < 0.05$ vs. control group; $^{**}P < 0.05$ vs. capecitabine-Oxali group; $^{***}P < 0.05$ vs. BV group.

HuIgG 4.0 mg/kg

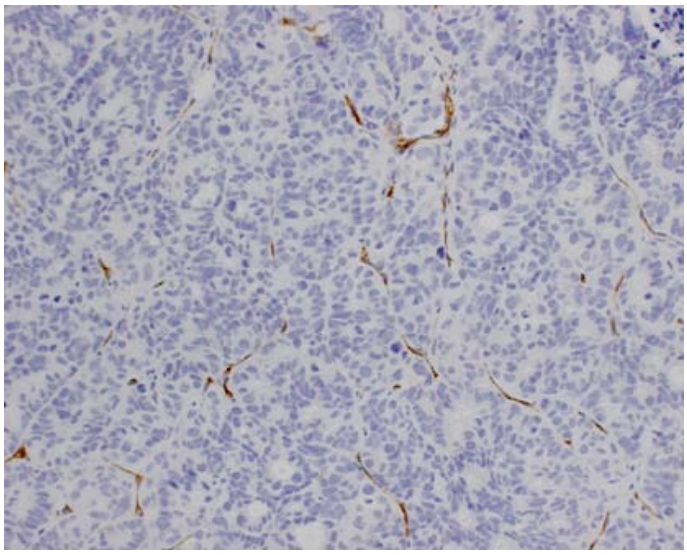

BV 4.0 mg/kg

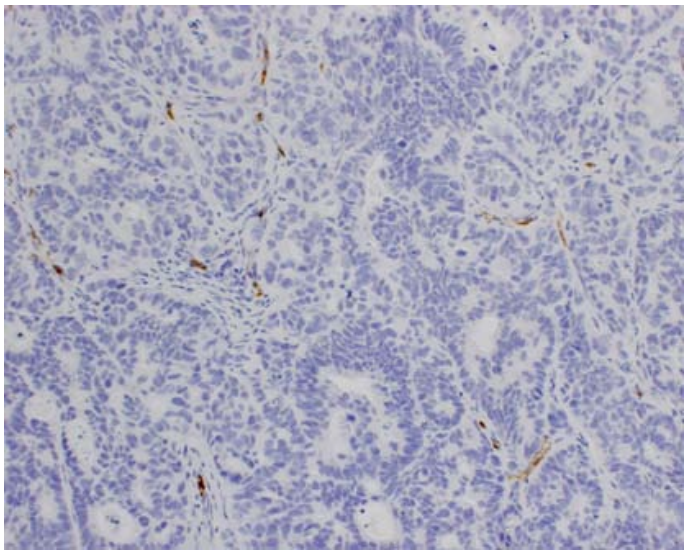

Figure 8. Images of CD34 staining for MVD in COL-16-JCK. Mice were randomly assorted into groups (n = 4). HuIgG or BV was administered i.p. twice a week for 3 weeks. Tumors were collected on Day 23 (5 days after the last treatment) and MVD was evaluated. Immunohistochemical staining for CD34 using the avidin-biotin-peroxidase complex method was performed on 4-μm thick sections of paraffin-embedded formalin-fixed tissue.

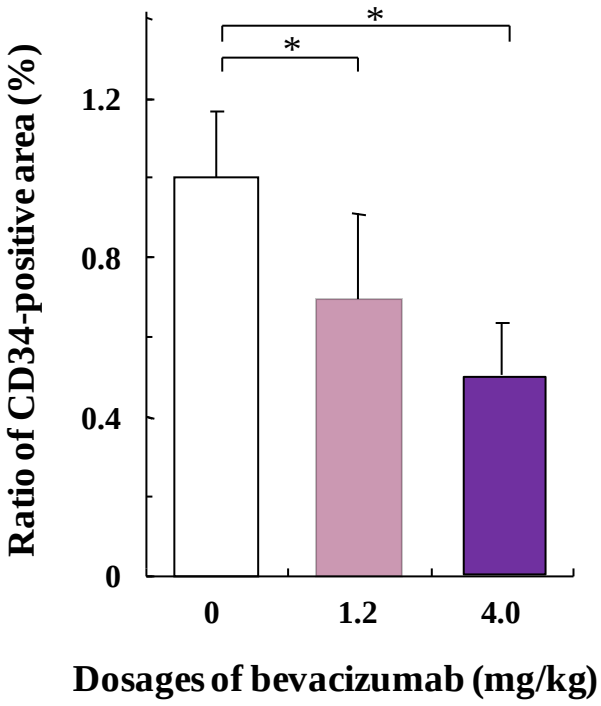

Figure 9. Effect of BV on MVD. HuIgG or BV was administered i.p. twice a week for 3 weeks. MVD was determined by the ratio of the CD34-positive area to the total observation area using imaging analysis software, Win ROOF. *P < 0.05 (n = 4).

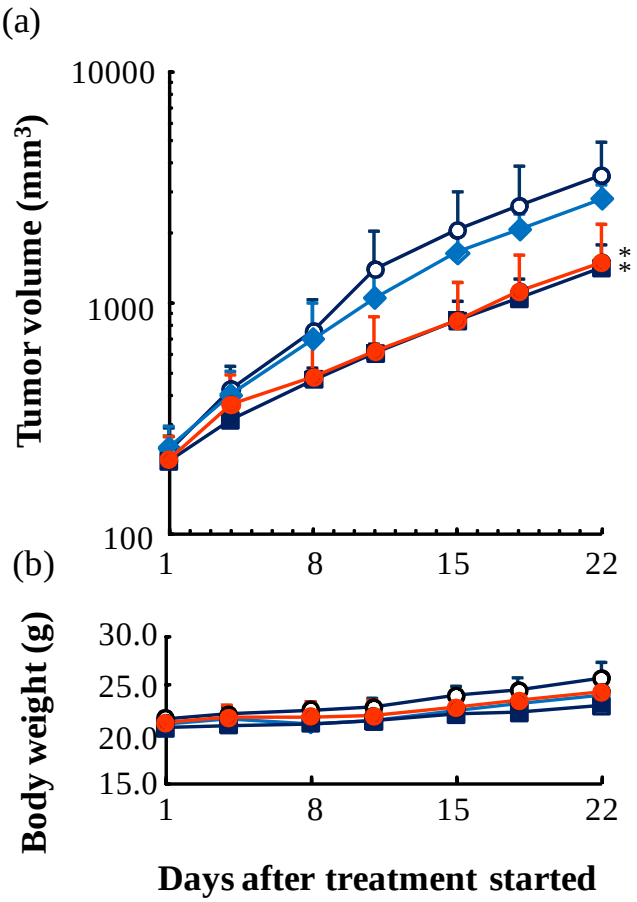

Figure 10 Antitumor activity of BV in the MX-1 human breast cancer xenograft model. Tumor volume change (a) and body weight change (b) were shown. Treatment was started 14 days after the tumor inoculation. Mice were randomly divided into four groups of six mice. Data points are mean plus standard deviation of tumor volume (mm^3). ○: control (HuIgG 20 mg/kg), ♦: BV 1.25 mg/kg, ■: BV 5 mg/kg, ●: BV 20 mg/kg. Asterisks indicate statistically significant differences. *$P \leq 0.05$ versus control group by Wilcoxon test.

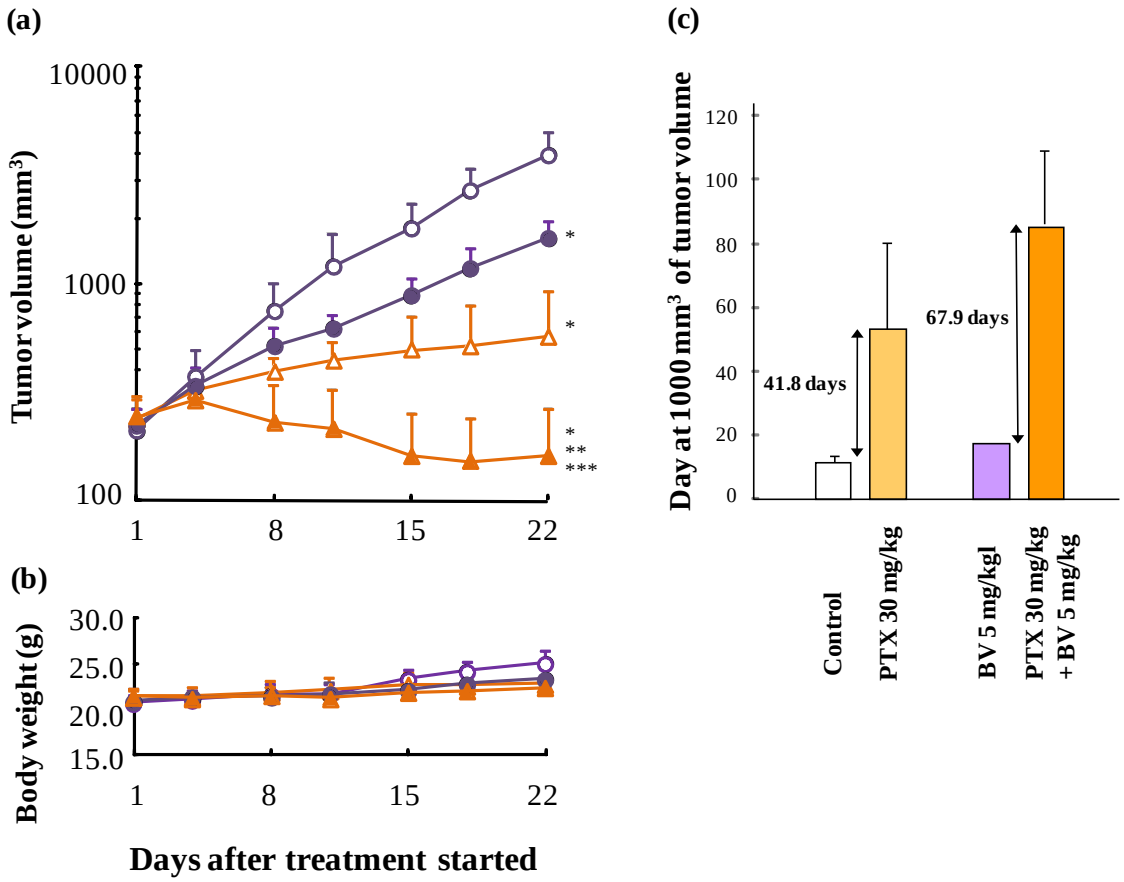

Figure 11. Antitumor activity of BV in combination with PTX in the MX-1 human breast cancer xenograft model. (a and b) Tumor volume and body weight in combination therapy with PTX-BV. Treatment was started 14 days after the inoculation of the tumor cells. Mice were randomly divided into four groups of six mice for the PTX-BV combination study. Data points: mean plus standard deviation (SD) of tumor volume (mm^3, a) or body weight (gram, b). ○: control group (HuIgG 5 mg/kg plus PTX vehicle), ●: BV group (BV 5 mg/kg plus PTX vehicle), Δ: PTX group (HuIgG 5 mg/kg plus PTX 20 mg/kg), ▲: combination group (BV 5 mg/kg plus PTX 20 mg/kg). Statistically significant differences are shown. *$P \leq 0.05$ versus control group, **$P \leq 0.05$ versus PTX group, ***$P \leq 0.05$ versus BV group by Wilcoxon test. (c) Tumor growth delay by BV treatment. Treatment was started 17 days after the inoculation of the tumor cells. Mice were randomly divided into four groups of six mice for the PTX-BV combination study. Bars: mean + SD of the day at 1000 mm^3 of tumor volume.

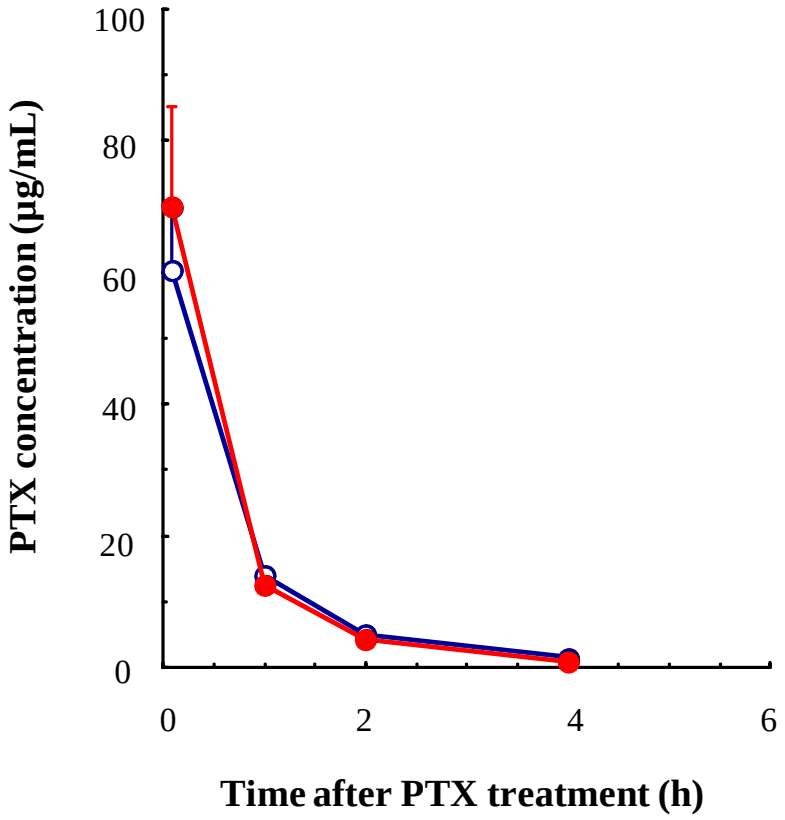

Figure 12. PTX concentration in plasma. ○, PTX group (PTX 30 mg/kg plus HuIgG 5 mg/kg); ●, PTX-BV group (PTX 30 mg/kg plus BV 5 mg/kg). Data points: mean + SD of PTX concentration (μg/mL). n = 6/group.

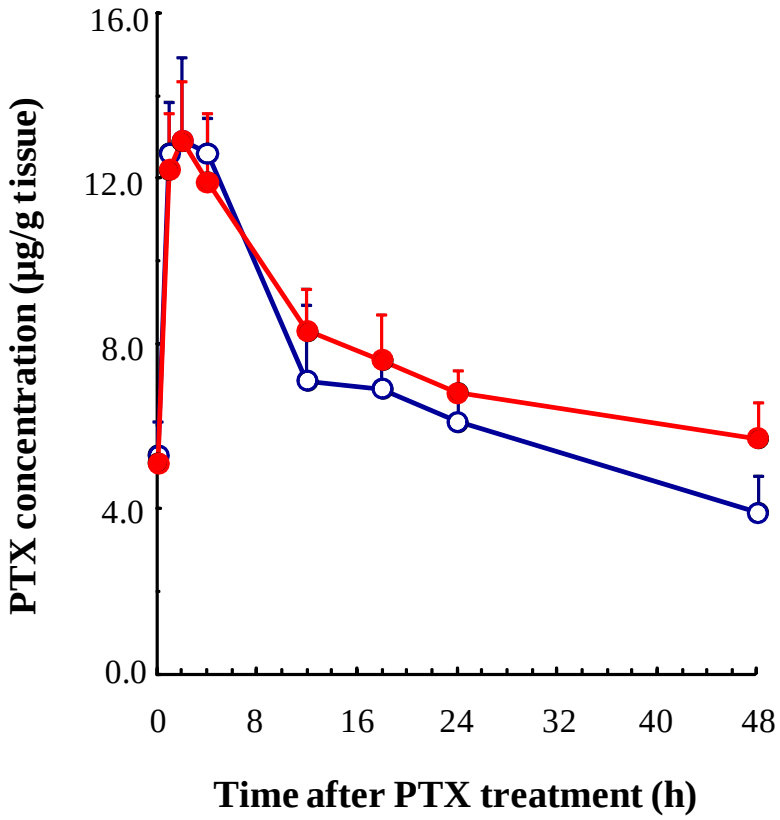

Figure 13. PTX concentration in tumor. ○, PTX group (PTX 30 mg/kg plus HuIgG 5 mg/kg); ●, PTX-BV group (PTX 30 mg/kg plus BV 5 mg/kg). Data points: mean + SD of PTX concentration (µg/g tissue). n = 6/group.

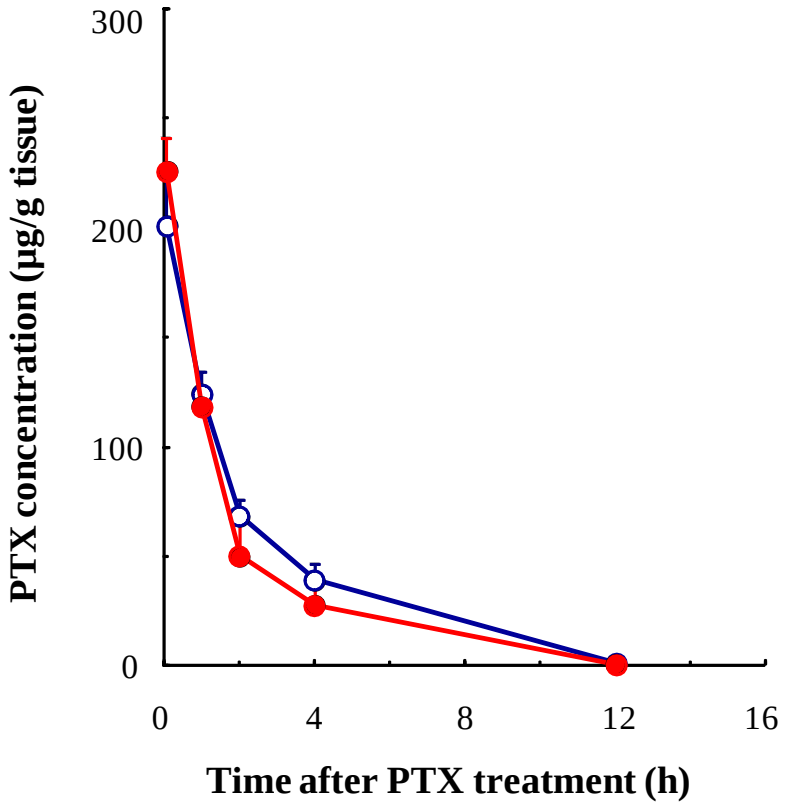

Figure 14. PTX concentration in liver. ○, PTX group (PTX 30 mg/kg plus HuIgG 5 mg/kg); ●, PTX-BV group (PTX 30 mg/kg plus BV 5 mg/kg). Data points: mean + SD of PTX concentration (μg/g tissue). n = 6/group.

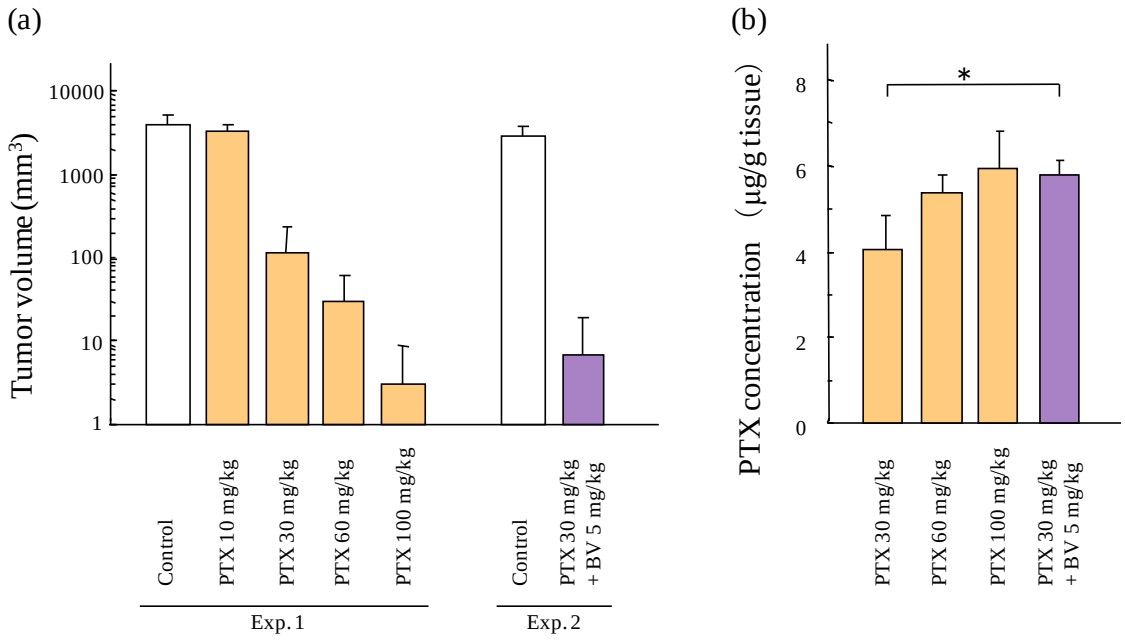

Figure 15. Comparison of PTX concentration in the tumor in MX-1 model. (a) Antitumor activity of PTX alone or PTX-BV in MX-1. Mice were randomly allocated to groups (n = 6/group). Bars: mean plus standard deviation of tumor volume (mm^3) on day 22. Tumor volume of the control group on day 1 in Experiments 1 and 2 was 185 ± 50 and 192 ± 77 mm^3, respectively. Tumor volume of the treatment group on day 1 was equivalent to the volumes for the control groups. (b) Concentration of PTX in the tumor. Mice were randomly allocated to four groups of six mice. PTX was administered intravenously 1 h after HuIgG or BV was administered intraperitoneally. Mice were sacrificed 48 h after the administration of PTX. The tumor was collected from each mouse and the PTX concentration was analyzed by high-performance liquid chromatography. *$P \leq 0.05$ versus PTX alone by the Wilcoxon test.

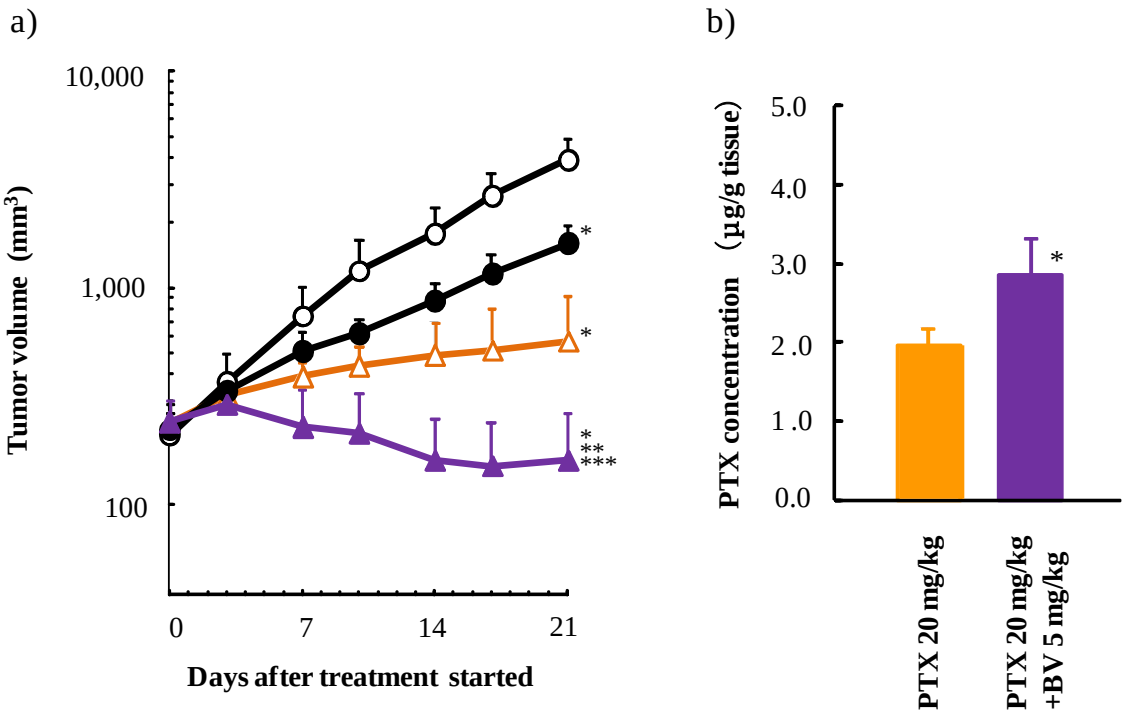

Fugure 16. Combination of BV with PTX and increased PTX in the tumor in the A549 model. (a) Antitumor activity of PTX-BV in A549. Mice were randomly allocated to groups (n = 8/group) 32 days after inoculation. Data points: mean plus standard deviation of tumor volume (mm^3). ○: control group (HuIgG 5 mg/kg plus PTX vehicle), ●: BV group (BV 5 mg/kg plus PTX vehicle), Δ: PTX group (HuIgG 5 mg/kg plus PTX 20 mg/kg), ▲: combination group (BV 5 mg/kg plus PTX 20 mg/kg). Statistically significant differences are shown. *P ≤ 0.05 versus control group, **P ≤ 0.05 versus PTX group, ***P ≤ 0.05 versus BV group by Wilcoxon test. (b) Concentration of PTX in the tumor. Mice were randomly allocated to two groups of six mice. PTX was administered intravenously 1 h after HuIgG or BV was administered intraperitoneally. Mice were sacrificed 48 h after the administration of PTX. The tumor was collected from each mouse and the PTX concentration was analyzed by high-performance liquid chromatography. *P ≤ 0.05 versus PTX alone by the Wilcoxon test.

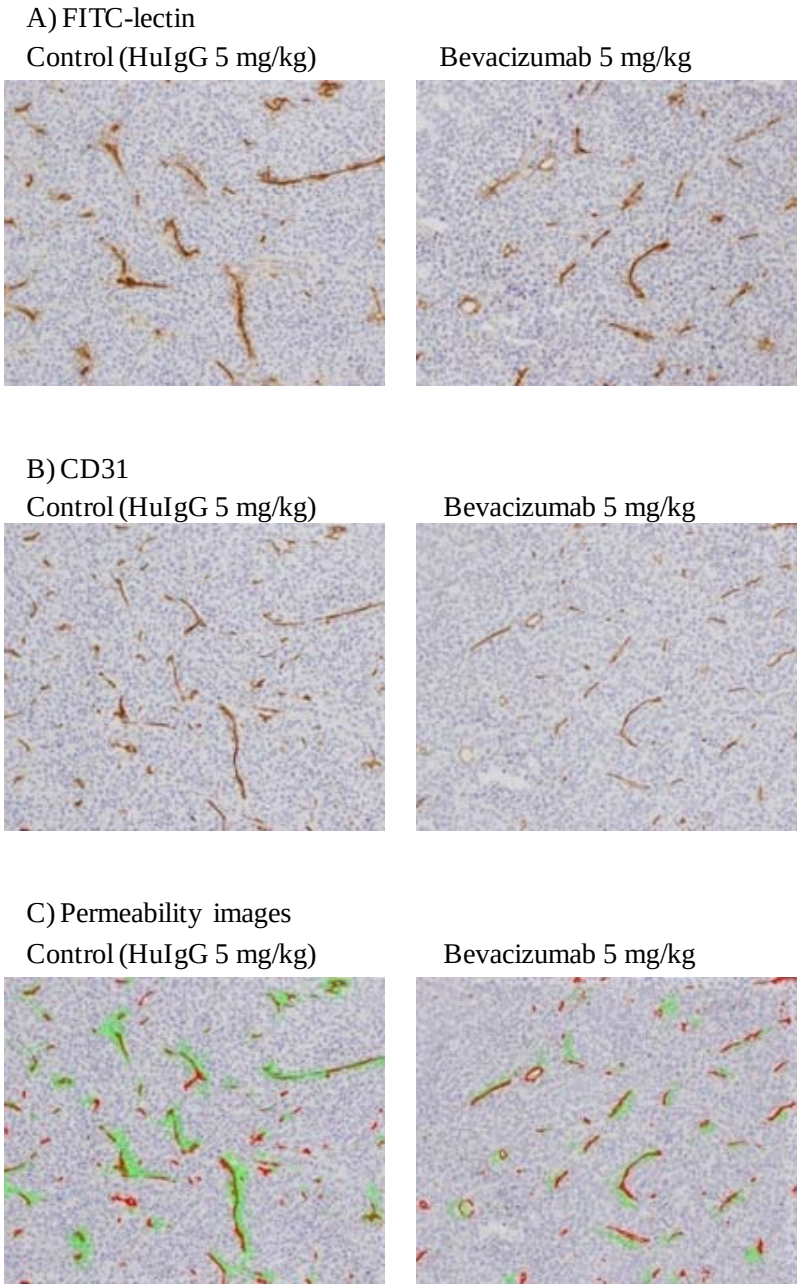

Figure 17. Immunohistochemical analysis of fluorescein isothiocyanate (FITC)–lectin and CD31. Mice were randomly divided into six groups of four mice. HuIgG or bevacizumab was administered intraperitoneally on day 1. Mice were sacrificed on day 2, day 5, or day 8. The tumors were collected from each mouse and the permeability in the tumor was determined from the difference between the area with CD31 positive staining and the area showing FITC-lectin-positive staining in adjacent tissue sections. The calculation of permeability was performed automatically by the imaging analysis software Win ROOF. Green area is FITC-lectin-positive staining and red area is CD31-positive staining in permeability images.

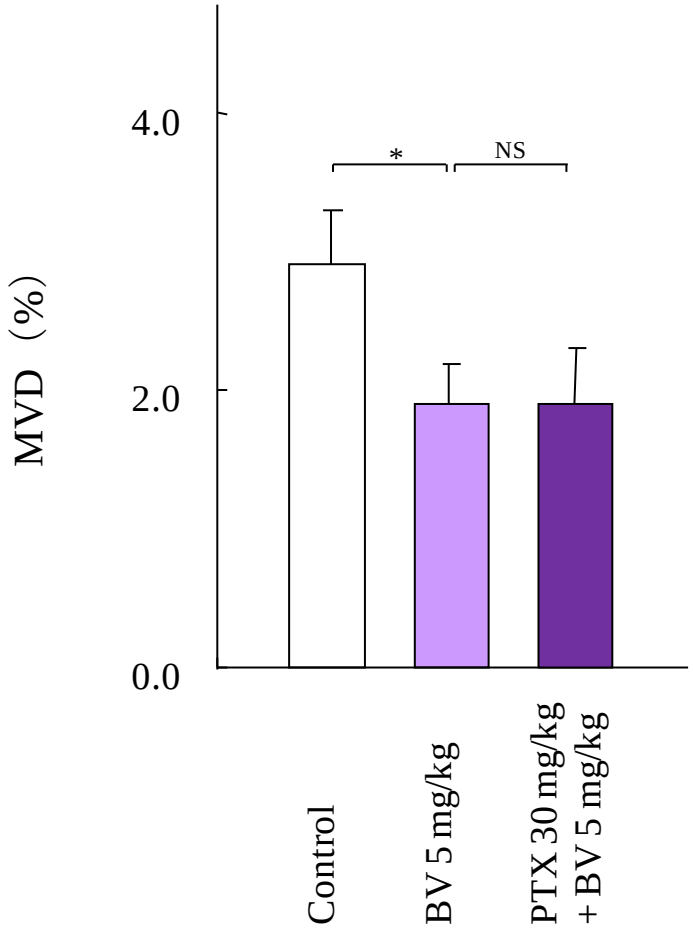

Figure 18. Effect of BV or PTX-BV on MVD. Mice were randomly allocated to groups (n = 4/group). PTX vehicle or PTX was administered intravenously on day 1. HuIgG 5 mg/kg (control) or BV 5 mg/kg was administered intraperitoneally on day 1. Mice were sacrificed on day 5. The tumors were collected from each mouse and the MVD was evaluated. *$P \leq 0.05$ versus control by the Wilcoxon test. NS, not significant.

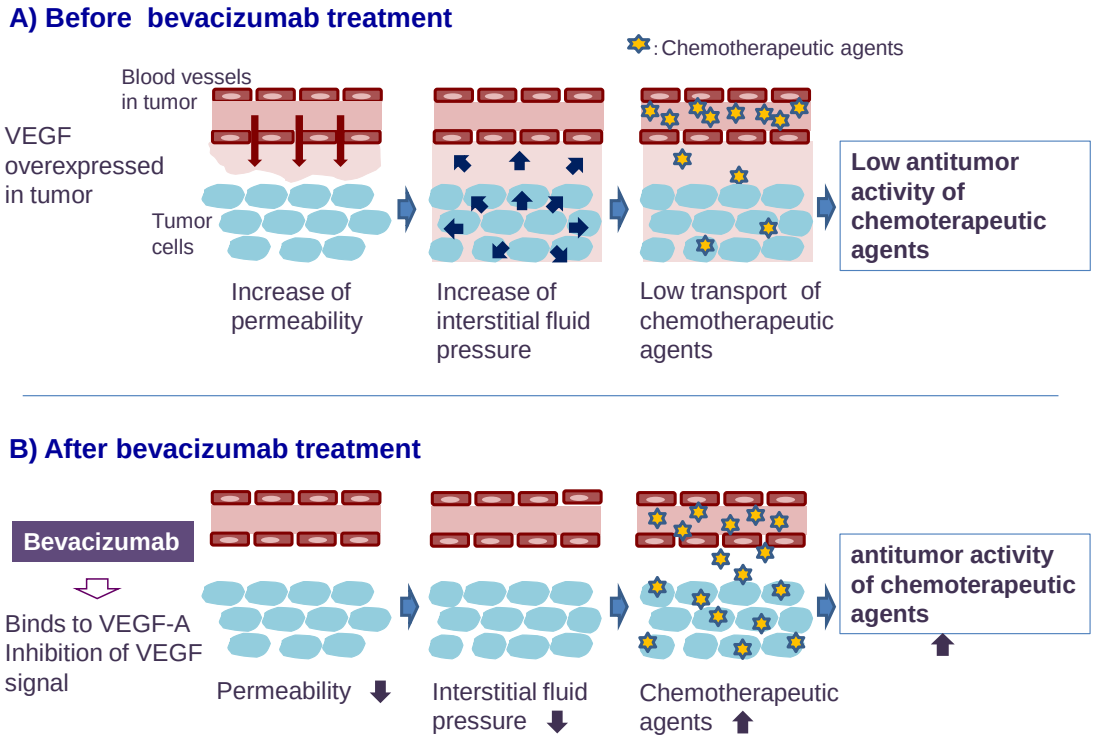

Figure 19. Hypothesis of how BV in combination with chemotherapy increases antitumor activity. In the tumor vessel, permeability is increased by VEGF and the plasma constituent leaks easily out of the blood vessel. Vascular permeability caused high IFP in tumor. Chemotherapeutic agents are difficult to transfer to tumor cells (A). When BV is treated, it binds to VEGF-A, and reduces the vascular permeability in tumor. IFP is declined and chemotherapeutic agents are transferred abundantly to tumor cells (B).